

**Donor-activated Alkali Metal Dipyridylamides:
Co-complexation Reactions with Zinc Alkyls and Reactivity
Studies with Benzophenone**

Supporting Information

**David R. Armstrong, Etienne V. Brouillet, Alan R. Kennedy, Jennifer. A. Garden,*
Markus Granitzka, Robert E. Mulvey,* Joshua J. Trivett**

*WestCHEM, Department of Pure and Applied Chemistry, University of Strathclyde,
Glasgow, G1 1XL. E-mail: r.e.mulvey@strath.ac.uk*

Table of Contents

1. Additional Crystallographic Information	4
1.1 Crystallographic Data	4
1.2 Molecular Structure of 3	5
2. NMR Spectra	6
2.1 NMR Spectra of 2 , 3 , 4 and [(TEMPO)Zn(^t Bu)]	6
2.2 DOSY Analysis of 1 , 2 , 3 and 4	21
3. Evaluating the Effect of Substituting ^t Bu ₂ Zn by ^t BuLi as the <i>tert</i> -Butyl Source	23
4. Neutral zinc complexes containing dpa ligands	24
5. DFT Calculations	29
5.1 [(PMDETA)Na(dpa)] ₂ , 2 _{calc}	29
5.2 [(H ₆ -TREN)Na(dpa)], 4 _{calc}	31
5.2.1 Total Energies (a.u.) and Relative Energies (kcal mol ⁻¹)	31
5.2.2 4 _{calc} - A (<i>syn-syn</i>)	32
5.2.3 4 _{calc} - B (<i>syn-anti</i>)	33
5.2.4 4 _{calc} - C (<i>anti-anti</i>)	34
5.3 [Zn(dpa) ₂], 6 _{calc}	35
5.3.1 Total Energies (a.u.) and Relative Energies (kcal mol ⁻¹)	35
5.3.2 [Zn(dpa) ₂], 6 _{calc} - A	36
5.3.3 [Zn(dpa) ₂], 6 _{calc} - B	37
5.3.4 [Zn(dpa) ₂], 6 _{calc} - C	38
5.3.5 [Zn(dpa) ₂], 6 _{calc} - D	38
5.3.6 [Zn(dpa) ₂], 6 _{calc} - E	40
5.4 [(TMEDA)Na(dpa)] ₂ , 8 _{calc}	41
6. Discussion of Dpa Bond Lengths and Bond Angles	42
7. Tables of Results	43
7.1 Donor Ligand Variation	43
7.1.1 Reactions with [(DMAP)Na(dpa)]	44
7.1.2 Reactions with [(TMEDA)Na(dpa)] ₂	45
7.1.3 Reactions with [(TMDAE)Na(dpa)] ₂	45
7.1.4 Reactions with [(PMDETA)Na(dpa)] ₂	46
7.1.5 Reactions with [(H ₆ -TREN)Na(dpa)]	47
7.1.6 Reactions with [(Me ₆ -TREN)Na(dpa)]	47
7.1.7 Reaction with [(TEMPO)Na(dpa)]	48
7.1.8 Reaction with [(PMDETA)Na(dpa)] ₂ and TEMPO	48
7.2 Variation of the Alkali Metal	49
7.3 Variation of the R Group: Reaction with Zn(CH ₂)Si(CH ₃) ₃	50
7.4 Variation of the Solvent System	51
7.5 Variation of the <i>tert</i> -butyl ligand source	53
References	54

Table of Figures

Figure S1 Molecular structure of 3 with thermal ellipsoids at 50% probability level ...	5
Figure S2 ¹ H NMR Spectrum of [(PMDETA)Na(dpa)] ₂ (2)	8
Figure S3 ¹³ C NMR Spectrum of [(PMDETA)Na(dpa)] ₂ (2)	8
Figure S4 DOSY NMR Spectrum of [(PMDETA)Na(dpa)] ₂ (2) with ^t Bu ₂ Zn	9
Figure S5 ¹ H NMR Spectrum of [(TMDAE)Na(dpa)] ₂ (3)	9
Figure S6 ¹³ C NMR Spectrum of [(TMDAE)Na(dpa)] ₂ (3)	10
Figure S7 DOSY NMR Spectrum of [(TMDAE)Na(dpa)] ₂ (3) with ^t Bu ₂ Zn	10
Figure S8 ¹ H NMR Spectrum of [(H ₆ -TREN)Na(dpa)] (4)	11
Figure S9 ¹³ C NMR Spectrum of [(H ₆ -TREN)Na(dpa)] (4)	11
Figure S10 DOSY NMR Spectrum of [(H ₆ -TREN)Na(dpa)] (4) with ^t Bu ₂ Zn	12
Figure S11 ¹ H NMR Spectrum of [(TEMPO)Zn(^t Bu)]	12
Figure S12 ¹³ C NMR Spectrum of [(TEMPO)Zn(^t Bu)]	13
Figure S13 Crude NMR Spectrum of 4- <i>tert</i> -butylbenzophenone and additional by-products.	13
Figure S14 Crude ¹ H NMR Spectrum of TEMPO- ^t Bu from the worked-up reaction of [(PMDETA)Na(dpa)] ₂ , ^t Bu ₂ Zn and TEMPO	14
Figure S15 Crude ¹³ C NMR Spectrum of TEMPO- ^t Bu from the worked-up reaction of [(PMDETA)Na(dpa)] ₂ , ^t Bu ₂ Zn and TEMPO	14
Figure S16 Reference ¹ H NMR Spectrum of commercially available dpaH in C ₆ D ₆ solvent.	15
Figure S17 Reference ¹ H NMR Spectrum of commercially available dpaH in d ₈ -THF .	15
Figure S18 Reference ¹ H NMR Spectrum of ^t Bu ₂ Zn in C ₆ D ₆	16
Figure S19 Reference ¹ H NMR Spectrum of ^t Bu ₂ Zn in d ₈ -THF.	16
Figure S20 Reference ¹ H NMR Spectrum of TMEDA in C ₆ D ₆	17
Figure S21 Reference ¹ H NMR Spectrum of TMEDA in d ₈ -THF.	17
Figure S22 ¹ H NMR Spectrum of [(PMDETA)Na(dpa)] in C ₆ D ₆ solvent.	18
Figure S23 ¹ H NMR Spectrum of [(PMDETA)Na(dpa)] with ^t Bu ₂ Zn in a 2:1 ratio.	18
Figure S24 ¹ H NMR Spectrum of [(TMDAE)Na(dpa)] in C ₆ D ₆ solvent.	19
Figure S25 ¹ H NMR Spectrum of [(TMDAE)Na(dpa)] with ^t Bu ₂ Zn in a 2:1 ratio.	19
Figure S26 ¹ H NMR Spectrum of [(H ₆ -TREN)Na(dpa)] in C ₆ D ₆ solvent.	20
Figure S27 ¹ H NMR Spectrum of [(H ₆ -TREN)Na(dpa)] with ^t Bu ₂ Zn in a 2:1 ratio.	20
Figure S28 Molecular structure of 6	26
Figure S29 Graphical representation of transition metal neutral dipyridylamine and anionic dipyridylamide complexes	27
Figure S30 Relative energies of DFT-modelled compounds 6 _{calc} - A-E	28

1. Additional Crystallographic Information

1.1 Crystallographic Data

Table S1 Crystallographic data and refinement details for compounds **2**, **3** and **6** (CCDC reference numbers 992383–992385).

	2	3	6
Empirical formula	C ₃₈ H ₆₂ N ₁₂ Na ₂	C ₃₆ H ₅₆ N ₁₀ Na ₂ O ₂	C ₂₀ H ₁₆ N ₆ Zn
Mol. Mass	732.98	706.89	405.76
Crystal system	Triclinic	orthorhombic	monoclinic
Space group	P -1	P bc2 ₁	C 2/c
<i>a</i> (Å)	10.3495(13)	15.8743(8)	22.5759(4)
<i>b</i> (Å)	11.0583(11)	12.4146(7)	9.5830(2)
<i>c</i> (Å)	18.5966(18)	19.8597(11)	16.0729(3)
α (°)	101.113(8)	90	90
β (°)	96.726(9)	90	99.734(2)
γ (°)	90.084(9)	90	90
<i>V</i> (Å ³)	2073.4(4)	3913.8(3)	3427.23(12)
<i>Z</i>	2	4	8
λ (Å)	1.5418	0.71073	1.54178
T (K)	123(2)	123(2)	123(2)
2 θ _{max} (°)	140.0	56.0	144.1
Measured reflections	17153	36891	10393
Unique reflections	17153	9425	3351
<i>R</i> _{int}	^a	0.0617	0.0186
Observed rflns [<i>I</i> > 2 σ (<i>I</i>)]	8270	6569	3102
GooF	1.167	1.014	1.074
<i>R</i> [on <i>F</i> , obs rflns only]	0.1510	0.0769	0.0344
<i>wR</i> [on <i>F</i> ² , all data]	0.4457	0.2266	0.1000
Largest diff. peak/hole/e Å ⁻³	0.862/-0.963	0.782/-0.671	0.565/-0.304
Flack	-	0.2(5)	-

^a Samples of **2** were not single crystals. Data was processed as twinned with the two parts related by matrix -0.9813 0.0624 0.0535 0.0681 1.0029 0.0203 -0.1850 -0.5925 -1.0129. The resulting HKLF 5 formatted file was used for refinement. BASF refined to 0.532(3).

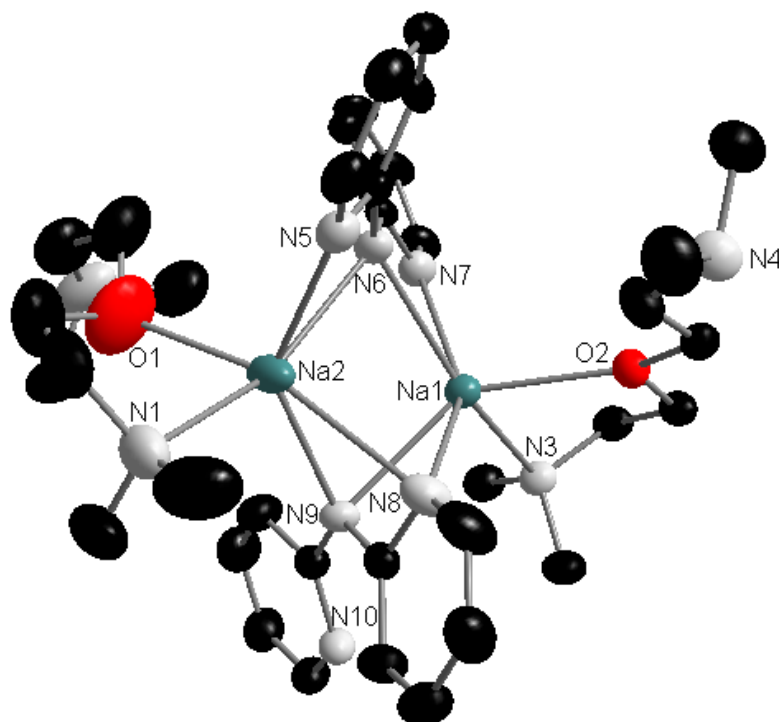
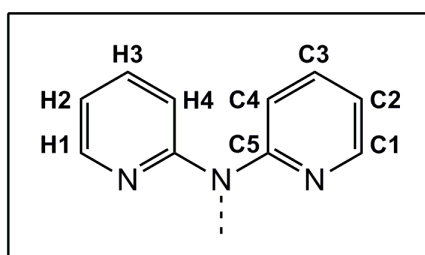
1.2 Molecular Structure of **3**

Figure S1 Molecular structure of **3** with thermal ellipsoids at 50% probability level. Hydrogen atoms and minor disordered components of TMDAE have been omitted for clarity. Selected bond lengths (Å) and bond angles (°): Na1-O2, 2.430(3); Na1-N3, 2.501(3); Na1-N6, 2.488(3); Na1-N7, 2.535(4); Na1-N8, 2.680(4); Na1-N9, 2.538(3); Na2-O1, 2.326(16); Na2-N1, 2.434(4); Na2-N5, 2.470(4); Na2-N6, 2.454(3); Na2-N8, 2.752(4); Na2-N9, 2.496(3); O2-Na1-N3, 71.06(10); O2-Na1-N6, 111.63(11); O2-Na1-N7, 102.93(11); O2-Na1-N8, 100.24(11); O2-Na1-N9, 139.81(11); N3-Na1-N6, 149.14(12); N3-Na1-N7, 94.91(12); N3-Na1-N8, 113.85(12); N3-Na1-N9, 93.47(11); N6-Na1-N7, 54.23(11); N6-Na1-N8, 96.23(12); N6-Na1-N9, 100.53(11); N7-Na1-N8, 147.69(12); N7-Na1-N9, 115.49(11); N8-Na1-N9, 51.39(10); O1-Na2-N1, 72.9(4); O1-Na2-N5, 101.4(4); O1-Na2-N6, 101.0(4); O1-Na2-N8, 163.7(4); O1-Na2-N9, 122.0(4); N1-Na2-N5, 100.85(14); N1-Na2-N6, 154.53(15); N1-Na2-N8, 93.33(14); N1-Na2-N9, 101.32(13); N5-Na2-N6, 55.34(12); N5-Na2-N8, 89.66(12); N5-Na2-N9, 135.37(13); N6-Na2-N9, 102.68(11); N6-Na2-N8, 95.21(12); N8-Na2-N9, 50.87(10); Na2-N6-Na1-N9, 15.281(2)[°]; Na1-N6-Na2-N8, 35.359(2)[°].

2. NMR Spectra

2.1 NMR Spectra of **2**, **3**, **4** and [(TEMPO)Zn(^tBu)]

Table S2 Comparison of ¹H (400.03 MHz, 300 K) and ¹³C{H} (100.59 MHz, 300 K) NMR shifts in *d*₈-THF solution for dpa(H) and its sodium derivatives [(PMDETA)Na(dpa)]₂ (**2**), [(TMDAE)Na(dpa)]₂ (**3**), [(H₆-TREN)Na(dpa)] (**4**).



Atom Assignment	dpa(H)	Chemical Shift (ppm)		
		2	3	4
H1	8.16	7.92	7.99	7.92
H2	6.75	6.20	6.38	6.22
H3	7.53	7.14	7.30	7.15
H4	7.72	7.07	7.30	7.15
C1	148.3	149.1	148.8	149.0
C2	116.3	110.3	112.3	109.9
C3	137.7	136.5	136.9	136.3
C4	112.5	112.5	112.6	113.0
C5	155.8	167.2	163.2	167.0

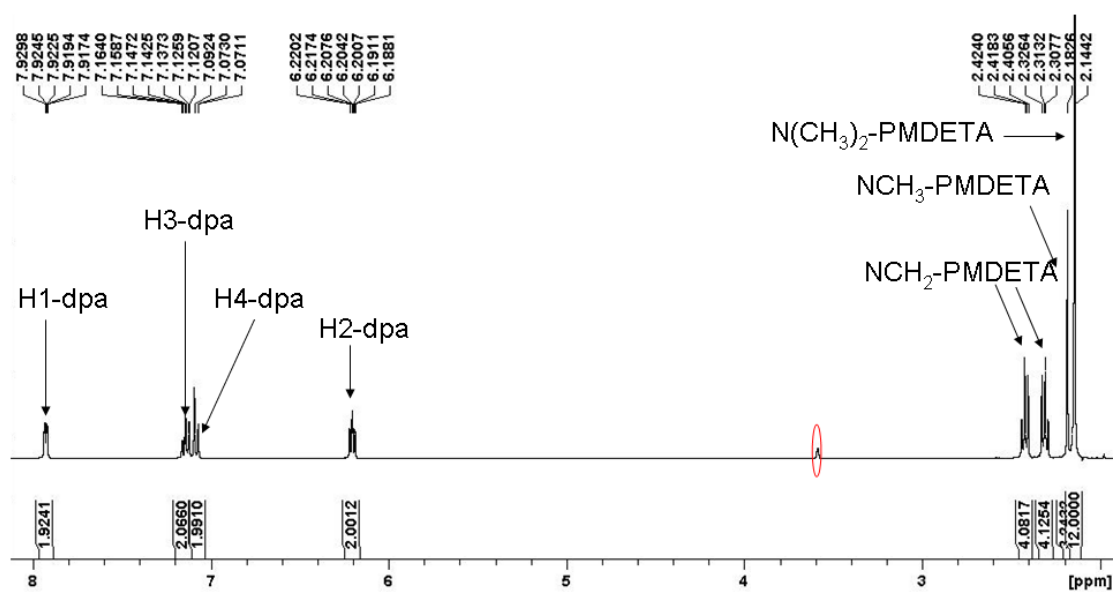
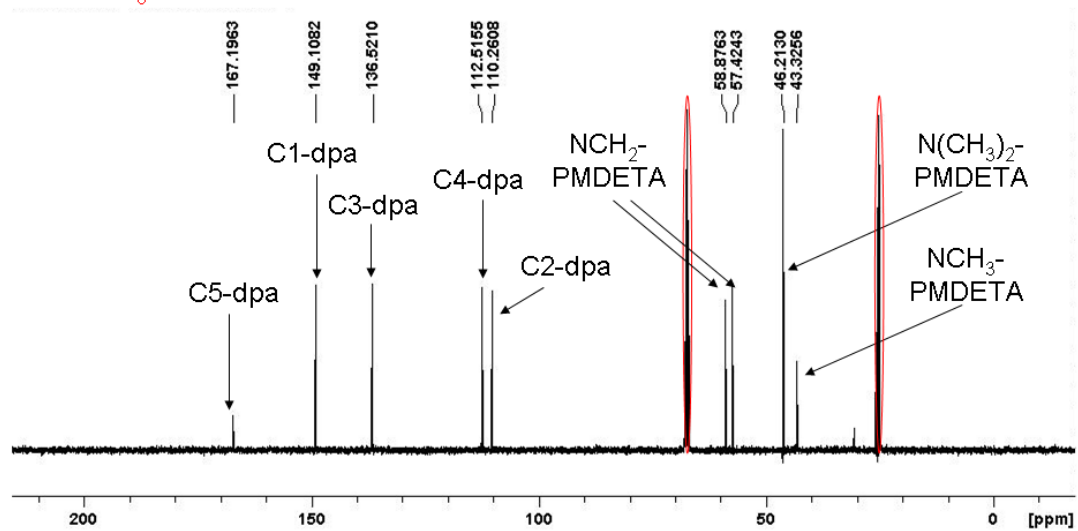
Table S3 Comparison of ^1H NMR data (400.03 MHz, 300 K, C_6D_6 solvent) for sodium amides **2**, **3** and **4**, in absence and presence of $^t\text{Bu}_2\text{Zn}$.

Signal	Chemical Shift (ppm)					
	2		3		4	
	[(PMDETA)Na(dpa)] ₂ without $^t\text{Bu}_2\text{Zn}$	[(PMDETA)Na(dpa)] ₂ with $^t\text{Bu}_2\text{Zn}$	[(TMDAE)Na(dpa)] ₂ without $^t\text{Bu}_2\text{Zn}$	[(TMDAE)Na(dpa)] ₂ with $^t\text{Bu}_2\text{Zn}$	[(TREN)Na(dpa)] without $^t\text{Bu}_2\text{Zn}$	[(TREN)Na(dpa)] With $^t\text{Bu}_2\text{Zn}$
H1-dpa	8.12	8.04	8.04	7.99	8.18	8.18
H2-dpa	6.31	6.30	6.26	6.26	6.34	6.33
H3-dpa	7.27	7.11	7.18	7.08	7.30	7.16
H4-dpa	7.15	7.11	7.09	7.07	7.20	7.05
$^t\text{Bu}_2\text{Zn}$	-	1.58	-	1.53	-	1.66
donor ^a	2.24	2.03	2.16	2.06	1.91	1.76
N(CH ₂)						
donor ^a	2.13	1.97	3.16	2.98	2.27	2.14
X(CH ₂) ^b						
donor ^a	2.11	1.92	2.01	1.92	0.78	0.58
NR ₂ ^c						
donor ^a	1.99	1.86	-	-	-	-
N(CH ₃)						

^a For **2**, donor = PMDETA, for **3**, donor = TMDAE, for **4**, donor = H₆-TREN ^b For **2** and **4**, X = N, for **3**, X = O ^c for **2** and **3**, R = (CH₃), for **4**, R = H.

Table S4 Comparison of ^1H NMR data (400.03 MHz, 300 K) for free TMEDA and TMEDA-coordinated zincate [{(TMEDA)Na(dpa)}₂Zn^tBu₂] (**1**).

Entry	Compound	Solvent	Chemical Shift (ppm)	
			CH ₂ - TMEDA	CH ₃ - TMEDA
1	TMEDA	C_6D_6	2.35	2.12
2	[{(TMEDA)Na(dpa)} ₂ Zn ^t Bu ₂] (1)	C_6D_6	1.69	1.74
3	TMEDA	<i>d</i> ₈ -THF	2.30	2.15
4	[{(TMEDA)Na(dpa)} ₂ Zn ^t Bu ₂] (1)	<i>d</i> ₈ -THF	2.30	2.15

solvent = d_8 THFFigure S2 ^1H NMR Spectrum of $[(\text{PMDETA})\text{Na}(\text{dpa})]_2$ (**2**).solvent = d_8 THFFigure S3 ^{13}C NMR Spectrum of $[(\text{PMDETA})\text{Na}(\text{dpa})]_2$ (**2**).

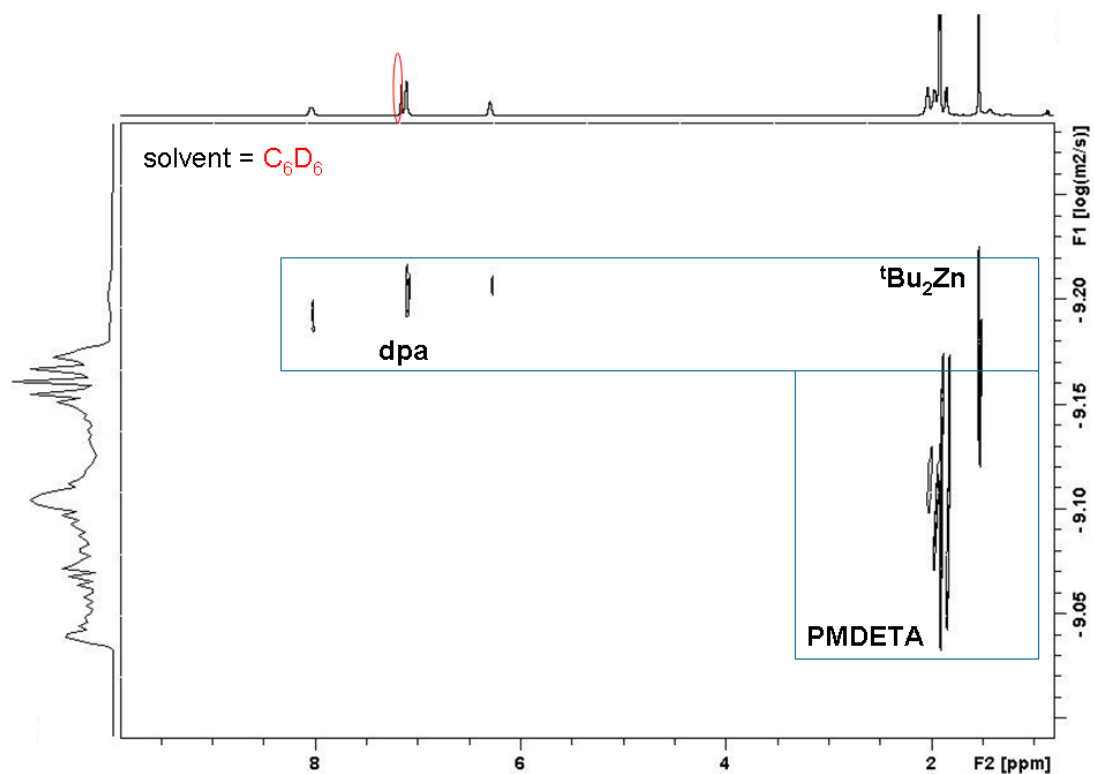


Figure S4 DOSY NMR Spectrum of $[(PMDETA)Na(dpa)]_2$ (**2**) with tBu_2Zn .

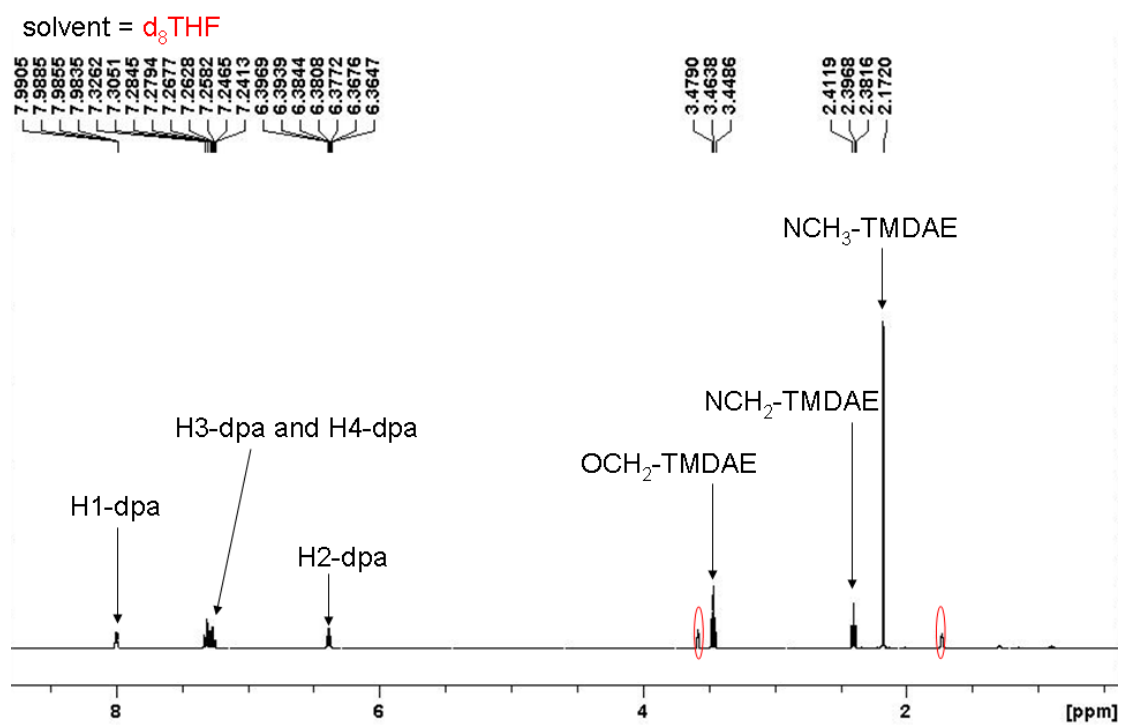
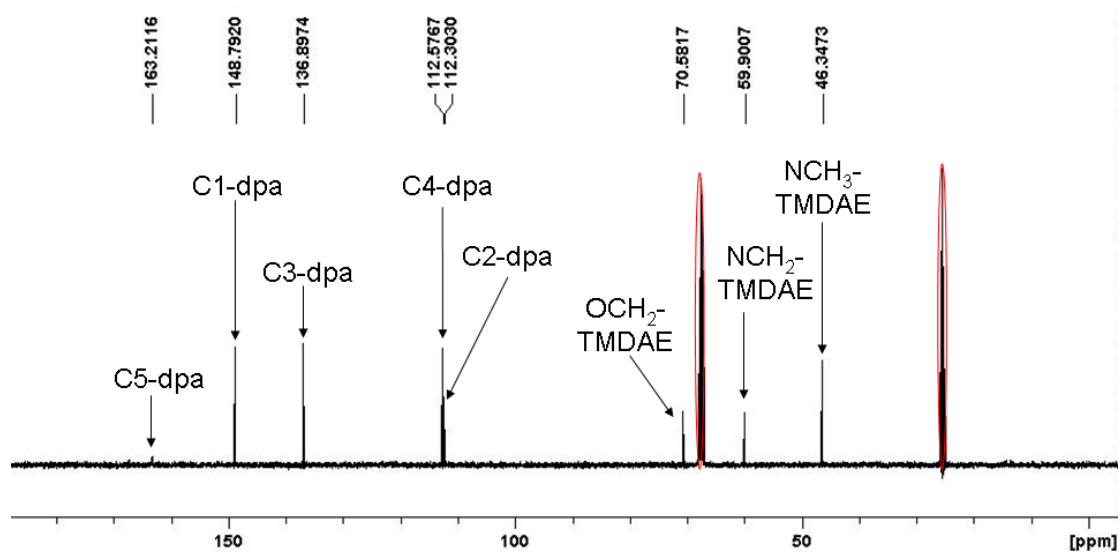
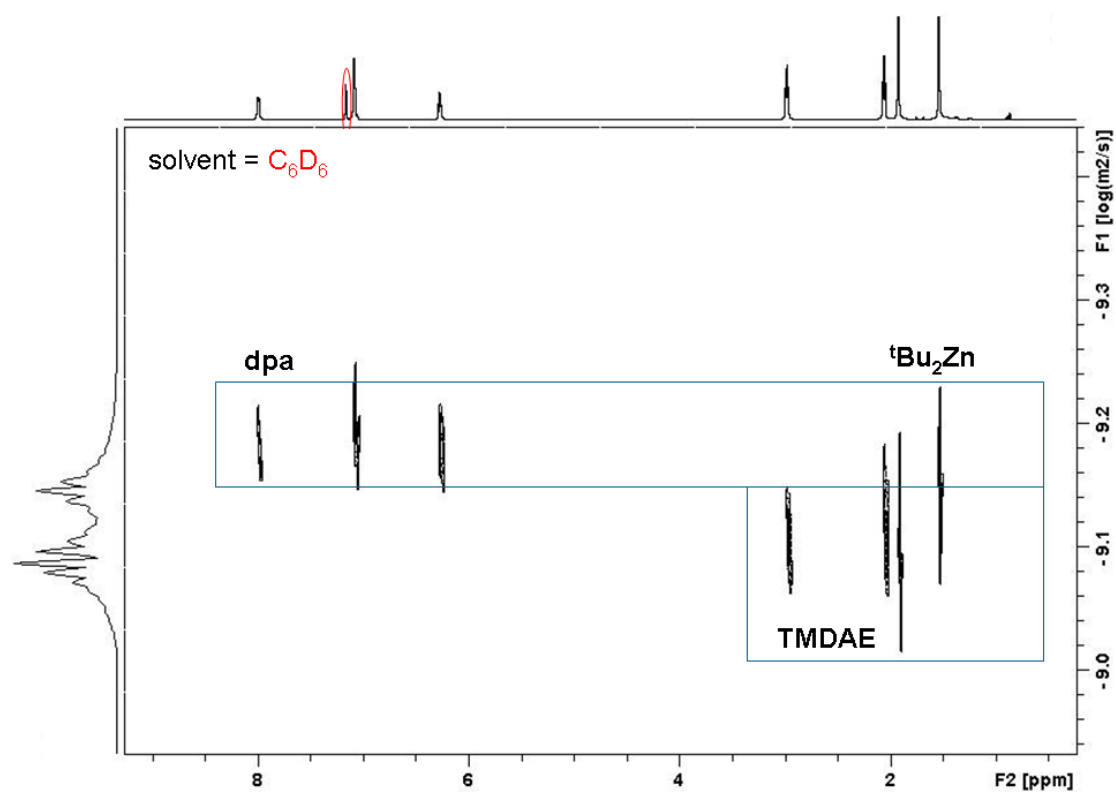
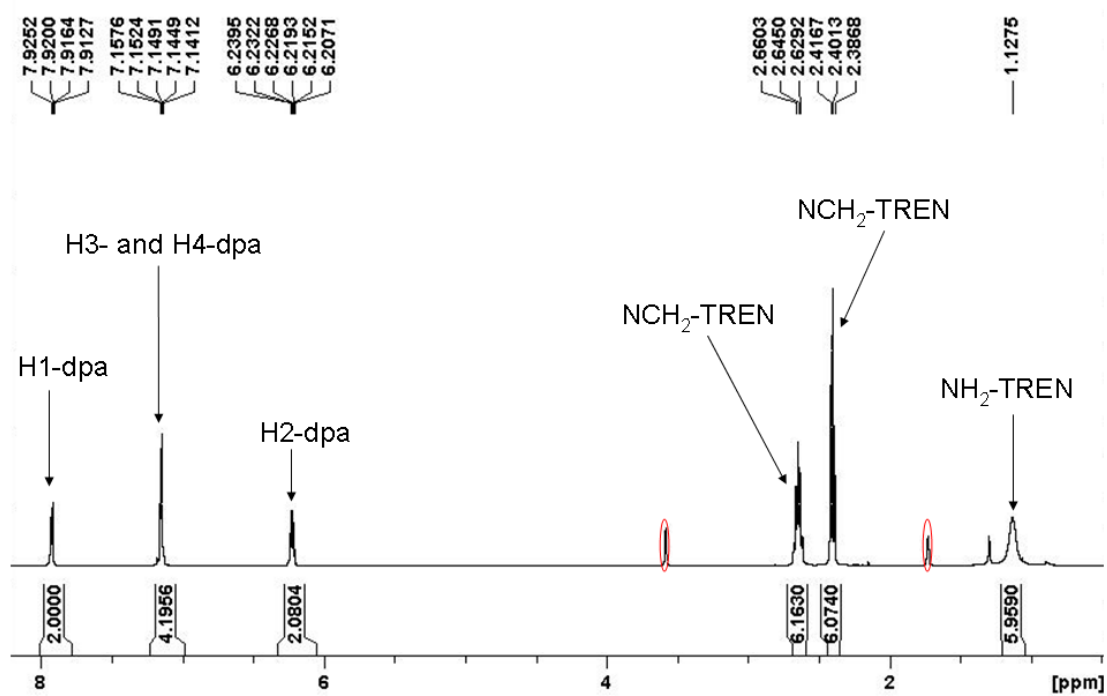
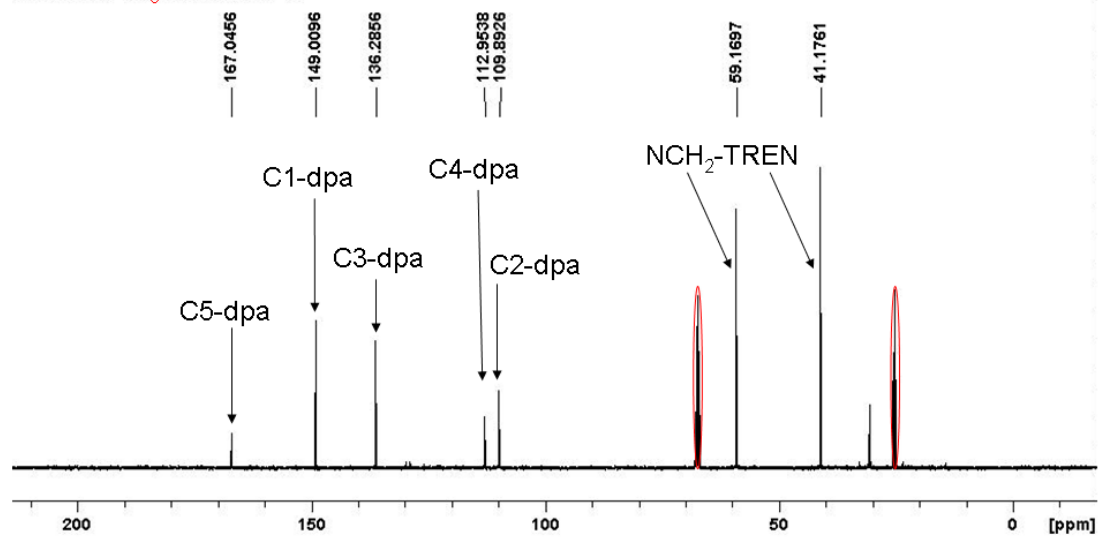


Figure S5 1H NMR Spectrum of $[(TMDAE)Na(dpa)]_2$ (**3**).

solvent = d_8 THFFigure S6 ^{13}C NMR Spectrum of $[(\text{TMDAE})\text{Na}(\text{dpa})]_2$ (**3**).Figure S7 DOSY NMR Spectrum of $[(\text{TMDAE})\text{Na}(\text{dpa})]_2$ (**3**) with $t\text{Bu}_2\text{Zn}$.

solvent = d_8 THFFigure S8 ¹H NMR Spectrum of [(H₆-TREN)Na(dpa)] (4).solvent = d_8 THFFigure S9 ¹³C NMR Spectrum of [(H₆-TREN)Na(dpa)] (4).

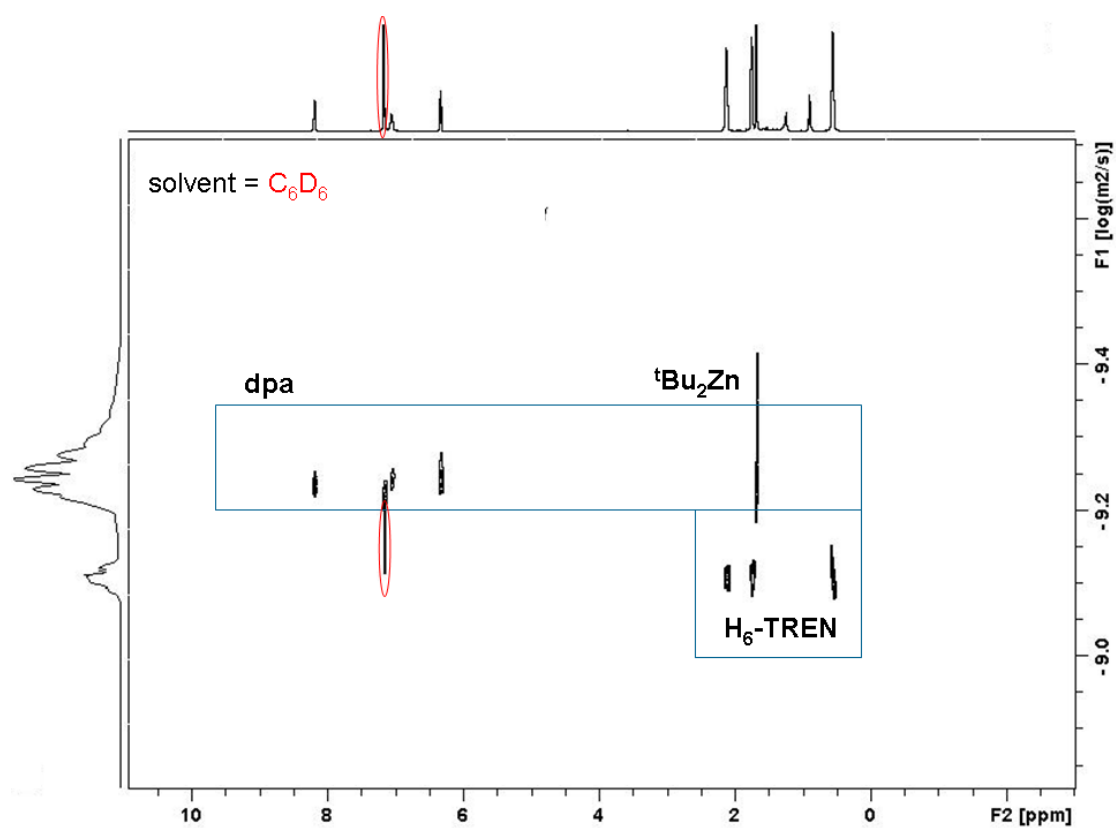


Figure S10 DOSY NMR Spectrum of $[(H_6-TREN)Na(dpa)]$ (4) with tBu_2Zn .

solvent = C_6D_6

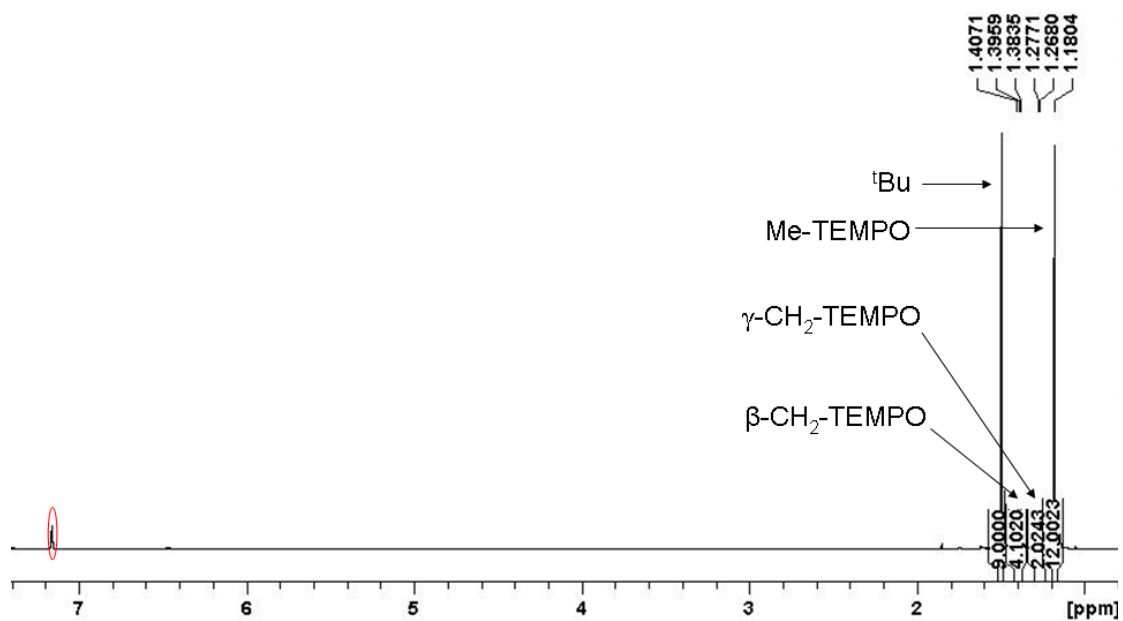
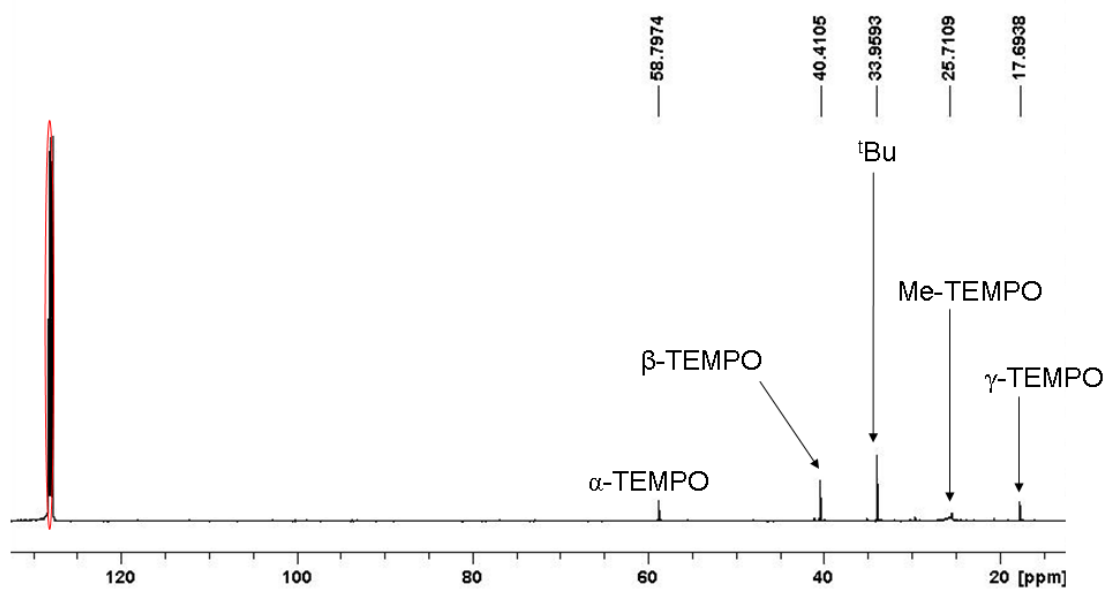
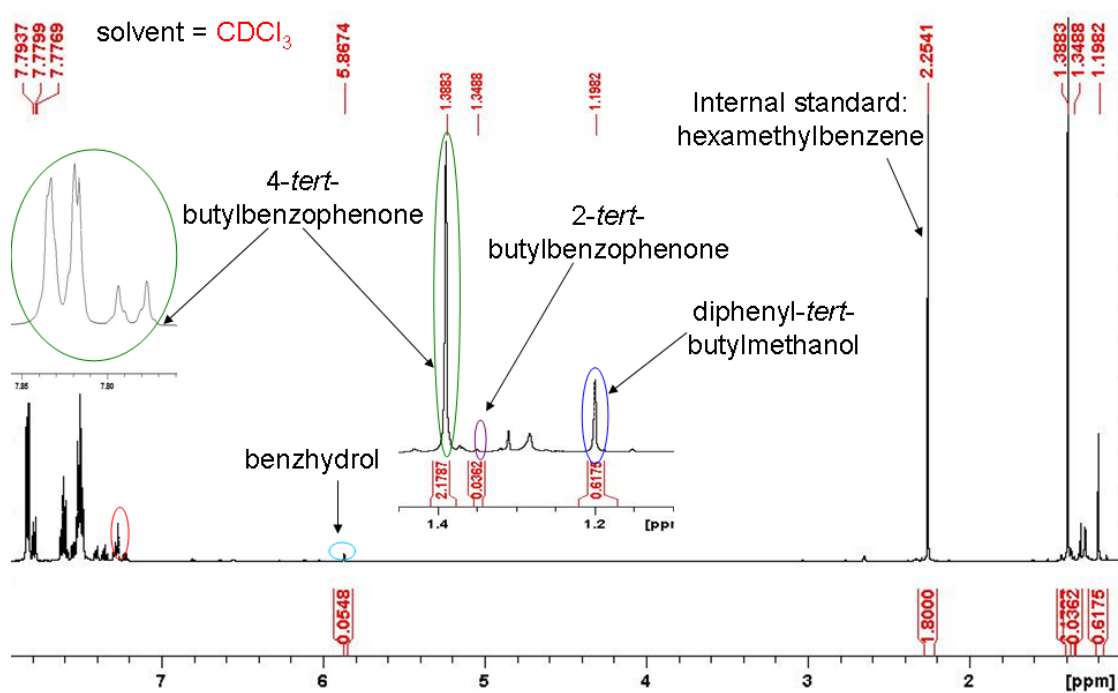


Figure S11 1H NMR Spectrum of $[(TEMPO)Zn(tBu)]$.

solvent = C_6D_6 Figure S12 ^{13}C NMR Spectrum of $[(TEMPO)Zn(tBu)]$.Figure S13 Crude NMR Spectrum of 4-*tert*-butylbenzophenone and additional by-products.

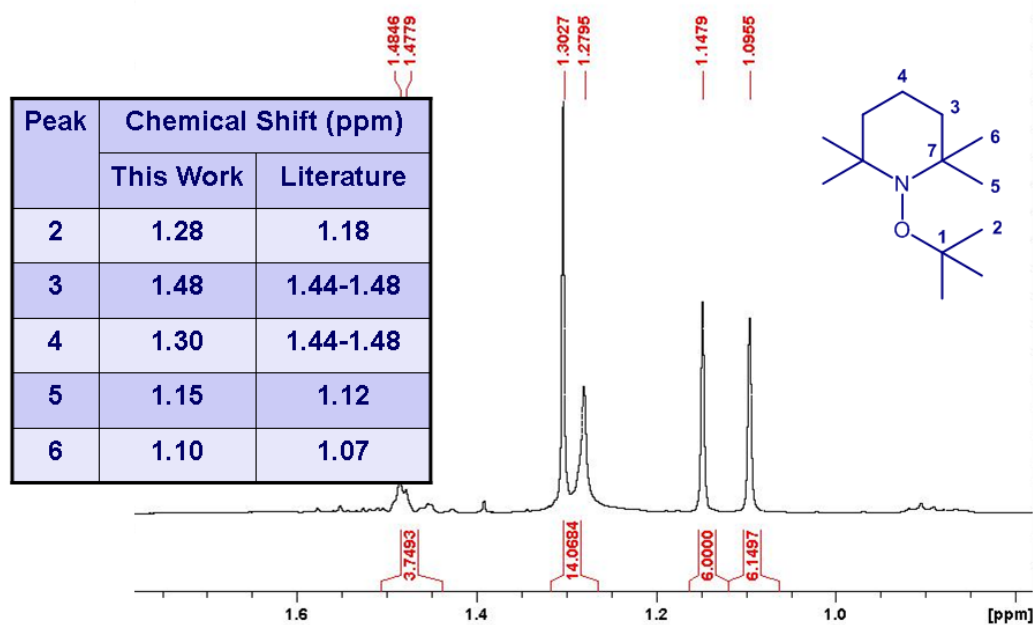


Figure S14 Crude ^1H NMR Spectrum of TEMPO- t Bu from the worked-up reaction of $[(\text{PMDETA})\text{Na}(\text{dpa})]_2$, $^t\text{Bu}_2\text{Zn}$ and TEMPO (comparison to literature values).¹ Assignments were verified by 2D COSY and HSQC experiments.

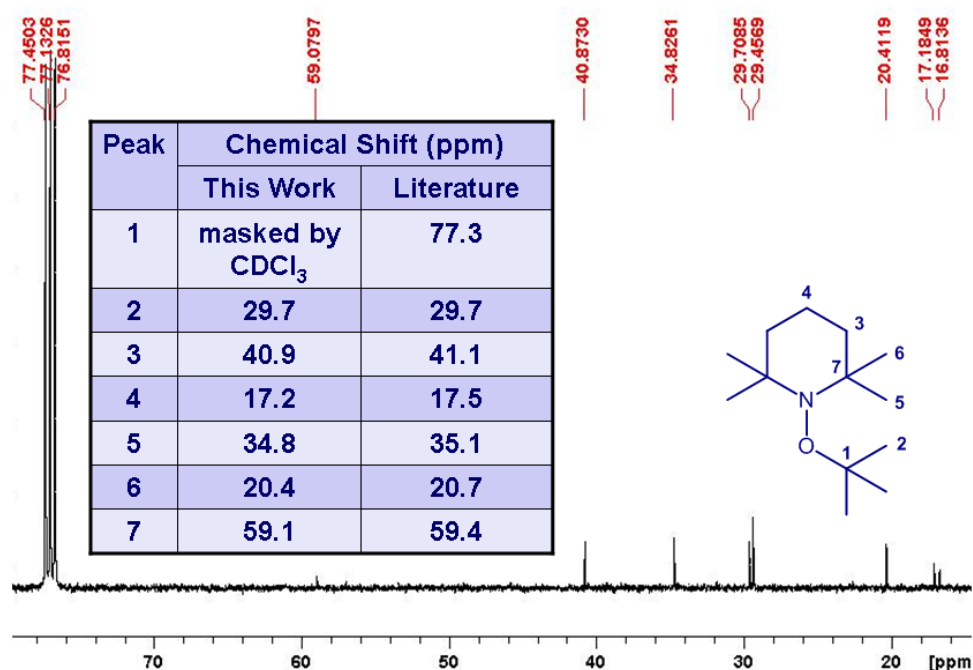


Figure S15 Crude ^{13}C NMR Spectrum of TEMPO- t Bu from the worked-up reaction of $[(\text{PMDETA})\text{Na}(\text{dpa})]_2$, $^t\text{Bu}_2\text{Zn}$ and TEMPO (comparison to literature values).¹ Assignments were verified by 2D COSY and HSQC experiments.

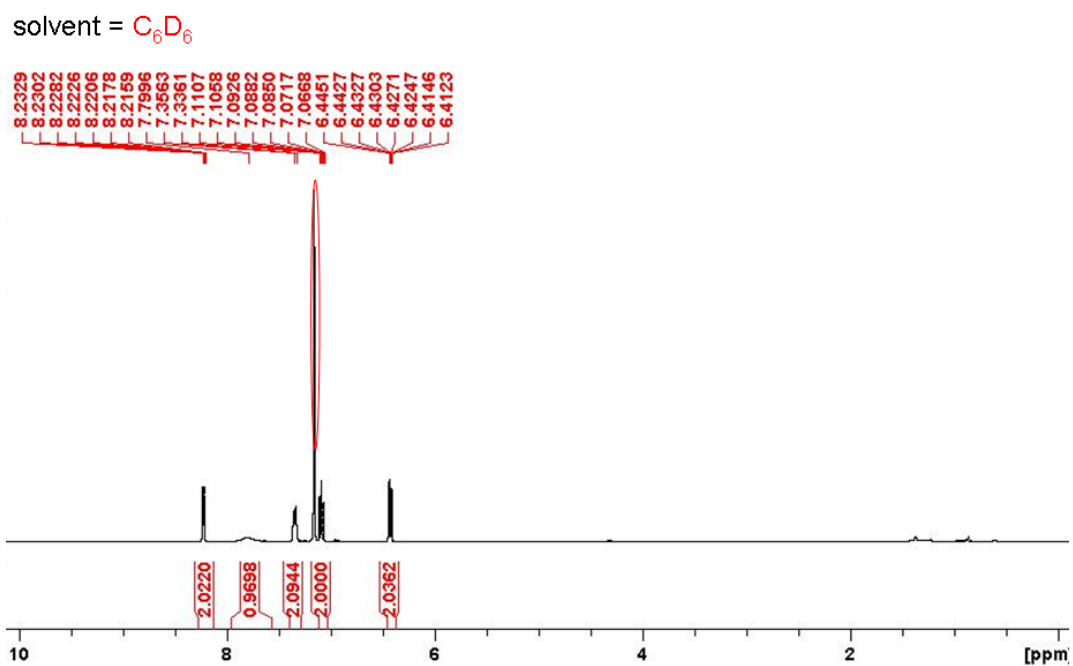


Figure S16 Reference ¹H NMR Spectrum of commercially available dpaH in C₆D₆ solvent.

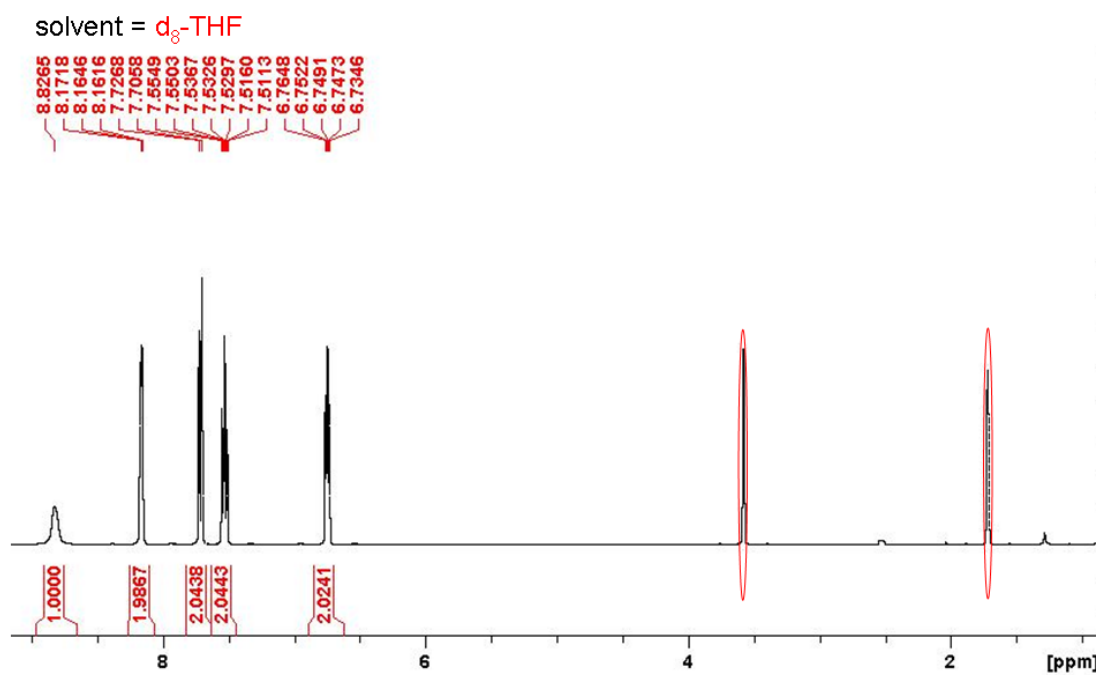
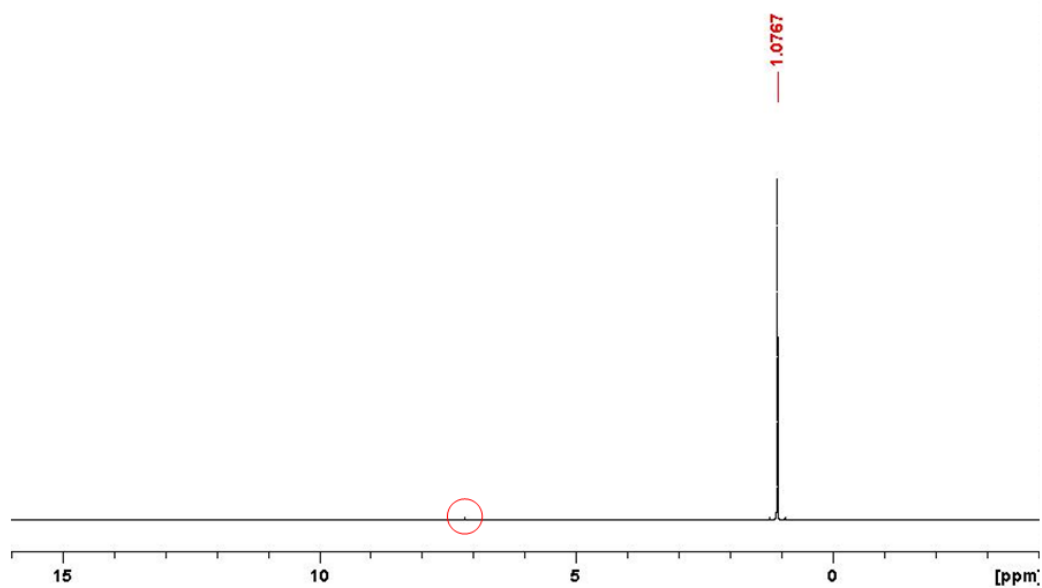
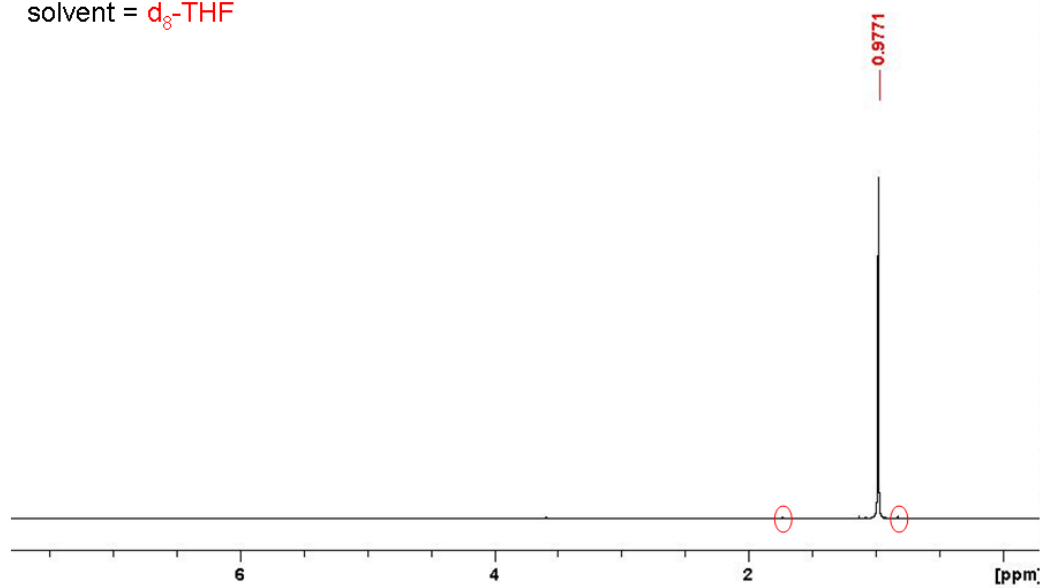
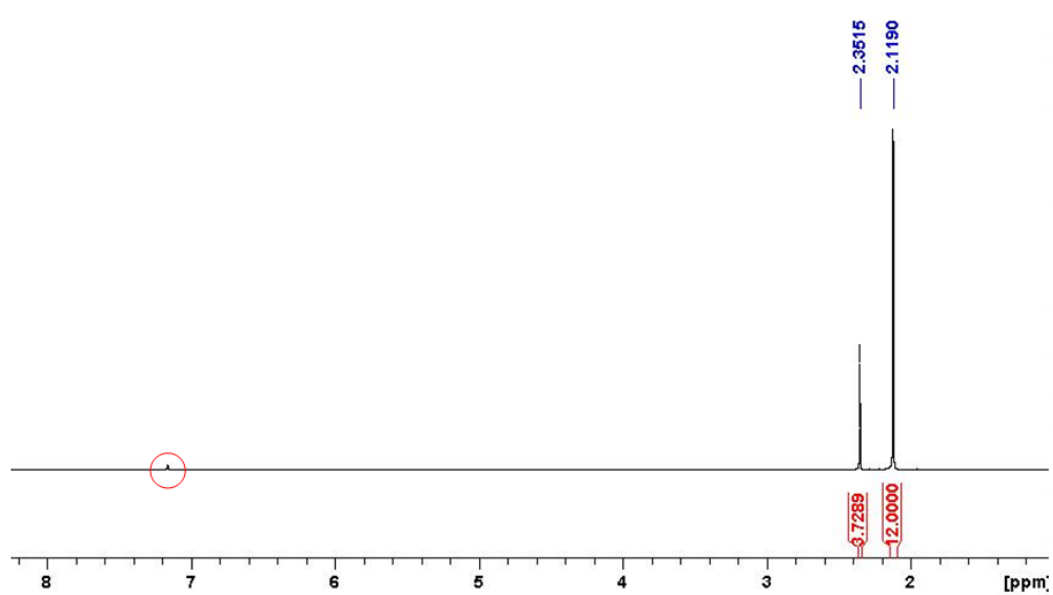
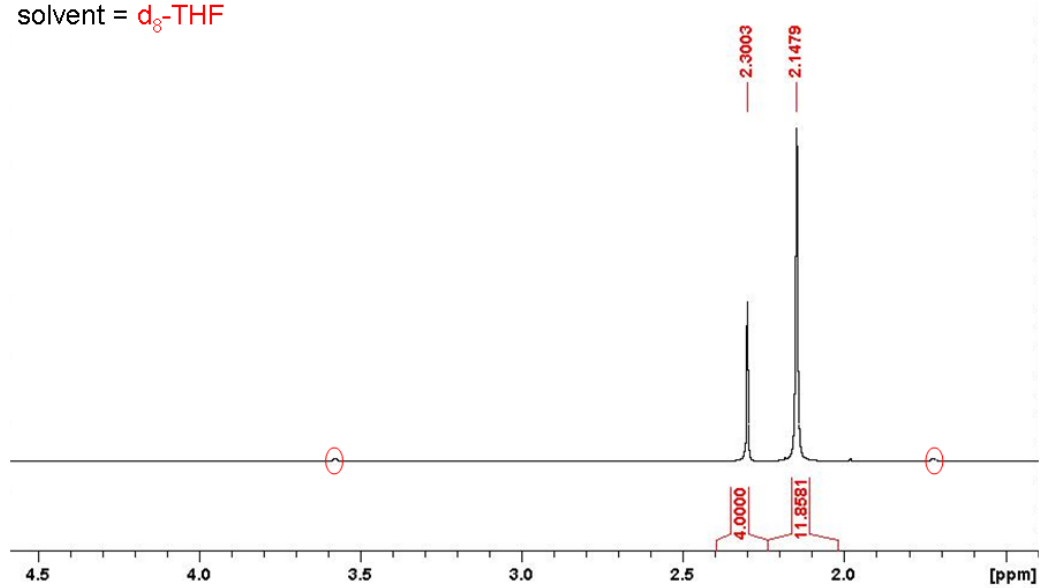


Figure S17 Reference ¹H NMR Spectrum of commercially available dpaH in d₈-THF.

solvent = C_6D_6 **Figure S18** Reference 1H NMR Spectrum of tBu_2Zn in C_6D_6 .solvent = d_8 -THF**Figure S19** Reference 1H NMR Spectrum of tBu_2Zn in d_8 -THF.

solvent = C_6D_6 Figure S20 Reference 1H NMR Spectrum of TMEDA in C_6D_6 .solvent = d_8 -THFFigure S21 Reference 1H NMR Spectrum of TMEDA in d_8 -THF.

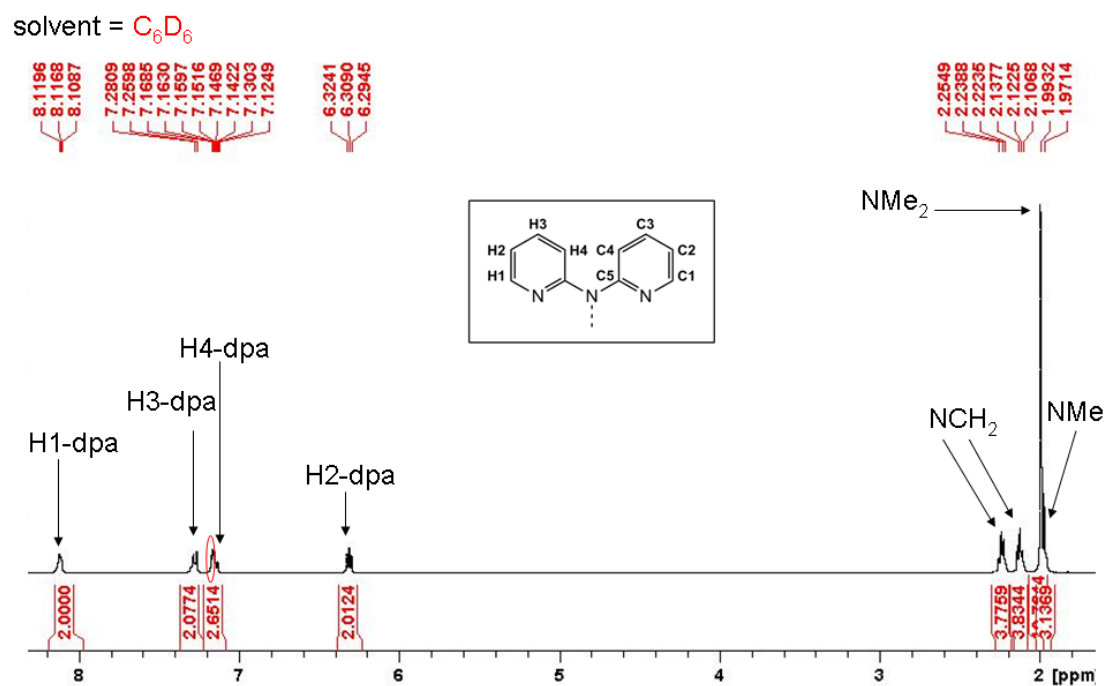


Figure S22 1H NMR Spectrum of $[(PMDETA)Na(dpa)]$ in C_6D_6 solvent.

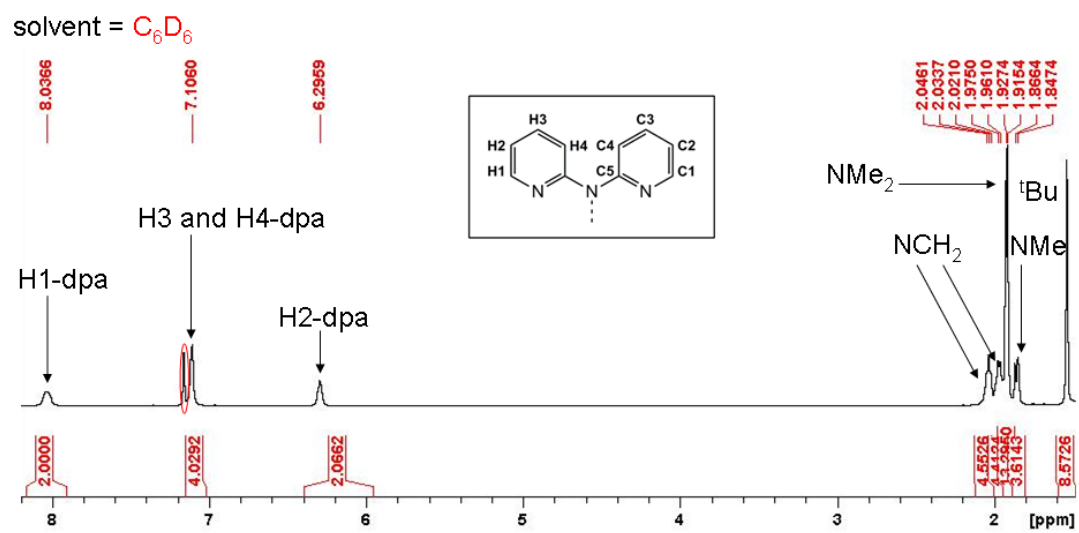


Figure S23 1H NMR Spectrum of $[(PMDETA)Na(dpa)]$ with tBu_2Zn in a 2:1 ratio.

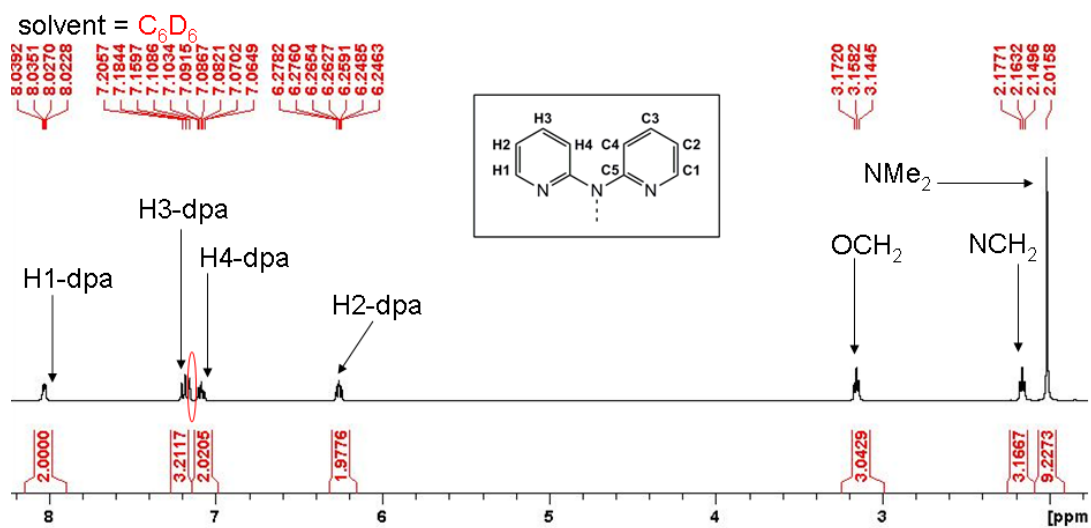


Figure S24 ¹H NMR Spectrum of [(TMDAE)Na(dpa)] in C₆D₆ solvent.

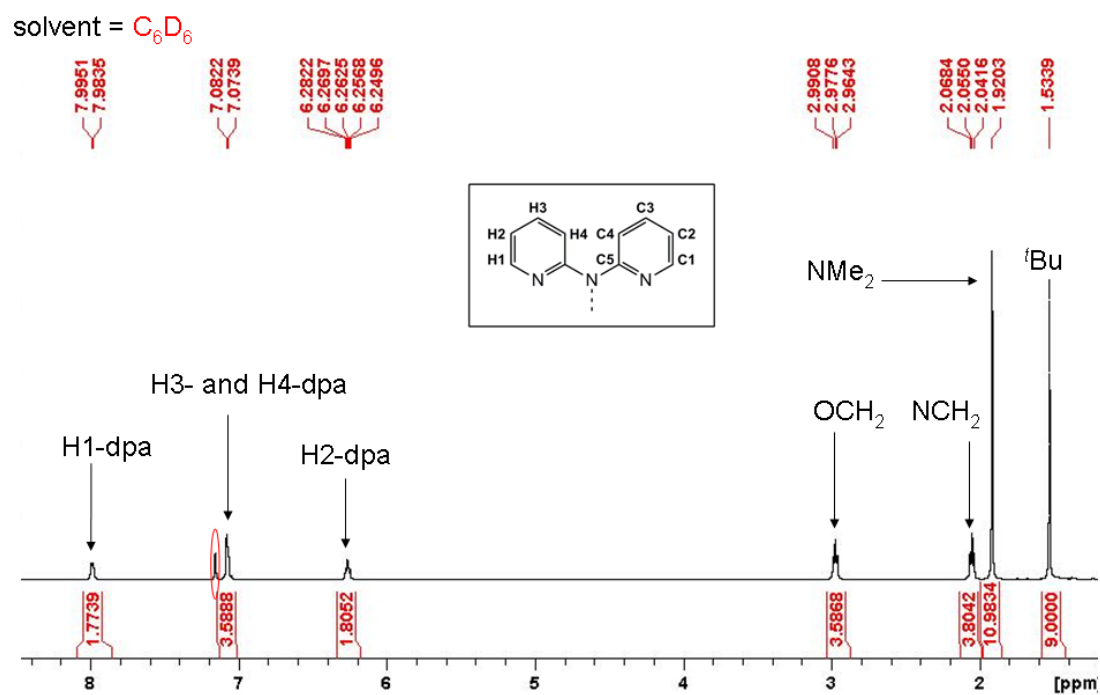


Figure S25 ¹H NMR Spectrum of [(TMDAE)Na(dpa)] with ^tBu₂Zn in a 2:1 ratio.

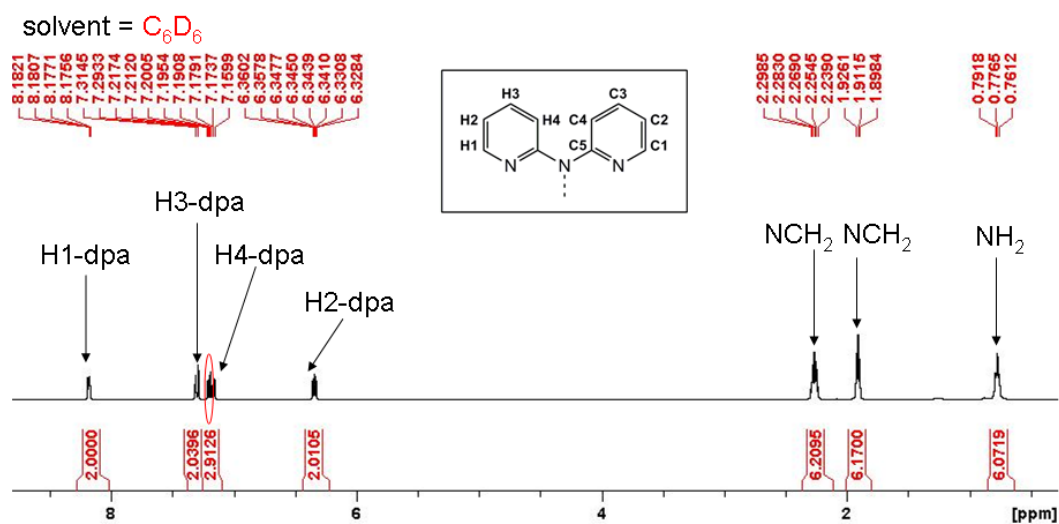


Figure S26 1H NMR Spectrum of $[(H_6-TREN)Na(dpa)]$ in C_6D_6 solvent.

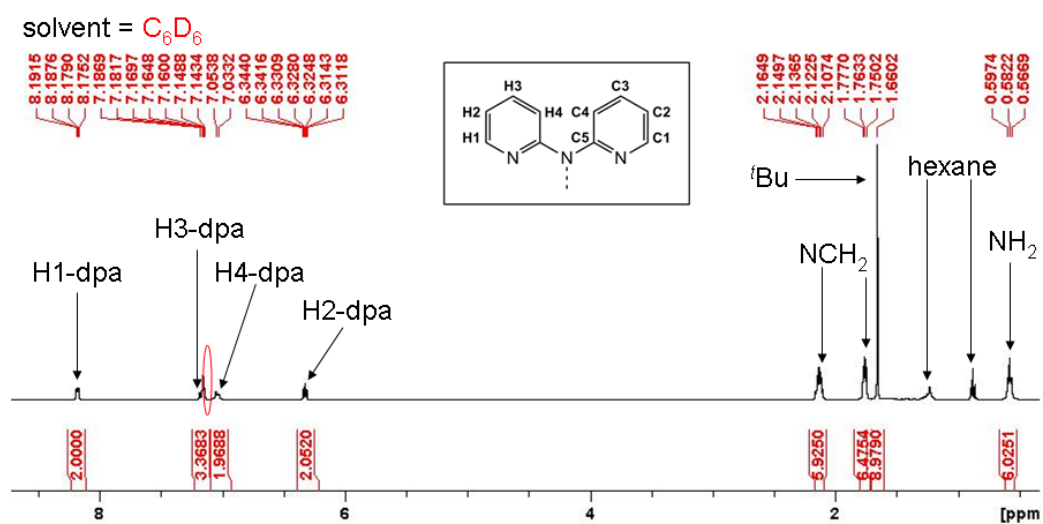


Figure S27 1H NMR Spectrum of $[(H_6-TREN)Na(dpa)]$ with tBu_2Zn in a 2:1 ratio.

2.2 DOSY Analysis of 1, 2, 3 and 4

To glean further insight into the solution state structure, we analysed these reaction systems by diffusion ordered spectroscopy (DOSY) experiments.²⁻⁴ The Diffusion-Ordered Spectroscopy (DOSY) NMR experiments were performed on a Bruker AVANCE 400 NMR spectrometer operating at 400.13 MHz for proton resonance under TopSpin (version 2.0, Bruker Biospin, Karlsruhe) and equipped with a BBFO-z-atm probe with actively shielded z-gradient coil capable of delivering a maximum gradient strength of 54 G/cm. Diffusion ordered NMR data was acquired using the Bruker pulse program dstegp3s employing a double stimulated echo with three spoiling gradients. Sine-shaped gradient pulses were used with a duration of 3 ms together with a diffusion period of 100 ms. Gradient recovery delays of 200 μ s followed the application of each gradient pulse. Data was accumulated by linearly varying the diffusion encoding gradients over a range from 2% to 95% of maximum for 64 gradient increment values. DOSY plot was generated by use of the DOSY processing module of TopSpin. Parameters were optimized empirically to find the best quality of data for presentation purposes.

A powerful and increasingly popular technique for the analysis of chemical mixtures,⁵⁻¹⁰ DOSY can shed light on the different species present in a multi-component solution, which are separated according to their diffusion coefficients. DOSY analysis of sodium amides **2-4** in the presence of ^tBu₂Zn establishes that the resonances attributed to dpa and ^tBu₂Zn possess similar diffusion coefficients (Table S6). For example, the resonances attributed to dpa-H4 and ^tBu₂Zn within **4** possess reasonably similar diffusion coefficients of $5.632 \times 10^{-10} \text{ m}^2 \text{ s}^{-1}$ and $5.580 \times 10^{-10} \text{ m}^2 \text{ s}^{-1}$ respectively, which points towards the coordination of **4** to ^tBu₂Zn in C₆D₆ solution. However, it is of note that the diffusion coefficients of donor ligands PMDETA, TMDAE and H₆-TREN differ significantly to those of dpa and ^tBu₂Zn. To demonstrate, the resonances of **4** assigned to H₆-TREN have diffusion coefficients ranging from 7.759 to $7.910 \times 10^{-10} \text{ m}^2 \text{ s}^{-1}$. As *d*₈-THF solvent has proven capable of displacing the donor ligands of **2**, **3** and **4** in solution (refer to manuscript), it seems likely that this

difference in diffusion coefficients could result from competitive equilibrium between donor ligand coordination and C₆D₆ coordination to Na. The capacity of benzene to act as a neutral π -donor towards sodium in the solid state has previously been observed through structural elucidation of the bimetallic complexes [(C₆H₆)NaCr{O-Si(^tBu)₃}₃]¹¹ and [(C₆H₆)NaAl(dpp-BIAN)Me₂] (where dpp-BIAN is 1,2-bis[(2,6-diisopropylphenyl)imino]acenaphthene).¹²

Table S5 Diffusion coefficients obtained from ¹H DOSY NMR experiment for [(TMEDA)Na(dpa)]₂^tBu₂Zn, **1**.

Chemical Shift (ppm)	Peak Assignment	Diffusion Coefficient D (10 ⁻¹⁰) m ² s ⁻¹
8.06	H1-dpa	6.169
7.06	H3- and H4-dpa	6.197
6.27	H2-dpa	6.164
1.71	CH ₃ -TMEDA	6.988
1.64	CH ₂ -TMEDA	7.062
1.56	^t Bu	6.734

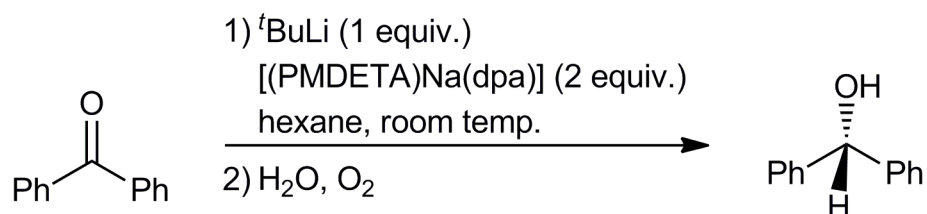
Table S6 Diffusion coefficients obtained from ¹H DOSY NMR experiments for sodium amides [(PMDTA)Na(dpa)]₂ (**2**), [(TMDAE)Na(dpa)]₂ (**3**) or [(H₆-TREN)Na(dpa)] (**4**) in combination with ^tBu₂Zn in C₆D₆ solution.

Signal	2 and ^t Bu ₂ Zn		3 and ^t Bu ₂ Zn		4 and ^t Bu ₂ Zn	
	δ (ppm)	Diffusion Coefficient (10 ⁻¹⁰) m ² s ⁻¹	δ (ppm)	Diffusion Coefficient (10 ⁻¹⁰) m ² s ⁻¹	δ (ppm)	Diffusion Coefficient (10 ⁻¹⁰) m ² s ⁻¹
dpa-H1	8.04	6.354	7.99	6.661	8.18	5.912
dpa-H2	6.30	6.097	6.26	6.655	6.34	5.766
dpa-H3	7.11	6.262	7.08	6.478	7.30	6.159
dpa-H4	7.11	6.262	7.07	6.478	7.20	5.632
^t Bu ₂ Zn	1.58	6.856	1.53	7.152	-	5.580
donor ^a N(CH ₂)	2.03	7.681	2.06	7.779	1.91	7.759
donor ^a X(CH ₂) ^b	1.97	8.142	2.98	7.864	2.27	7.839
donor ^a NR ₂ ^c	1.92	7.821	1.92	8.135	0.78	7.910
donor ^a N(CH ₃)	1.86	7.515	-	-	-	-

^a For **2**, donor = PMDETA, for **3**; donor = TMDAE; for **4**, donor = H₆-TREN ^b for **2** and **4**, X = N; for **3**, X = O ^c for **2** and **3**, R = (CH₃); for **4**, R = H.

3. Evaluating the Effect of Substituting ${}^t\text{Bu}_2\text{Zn}$ by ${}^t\text{BuLi}$ as the *tert*-Butyl Source

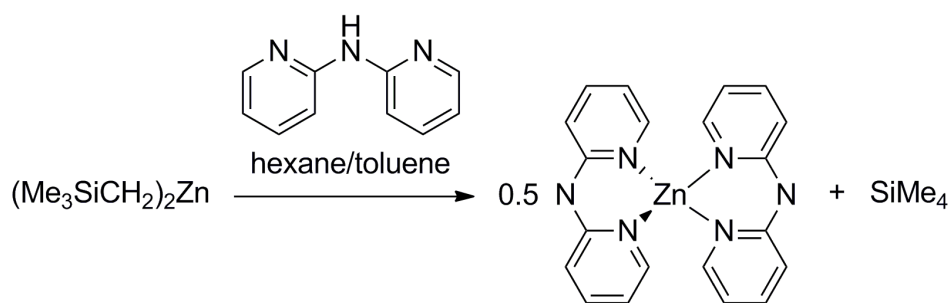
The effect of substituting ${}^t\text{Bu}_2\text{Zn}$ by ${}^t\text{BuLi}$ as the *tert*-butyl source was also evaluated. It was found that substituting ${}^t\text{Bu}_2\text{Zn}$ by ${}^t\text{BuLi}$ as the *tert*-butyl ligand source in combination with $[(\text{PMDETA})\text{Na}(\text{dpa})]$ shuts down any *para*-addition, with the yield falling from 48% to 0%. Moreover, no other *tert*-butylation products were observed. Only recovered benzophenone and the hydride addition product benzhydrol were obtained, with benzhydrol obtained in low but variable yields ranging from 16% to 32% (Scheme S1).¹³ A more ferocious reagent than ${}^t\text{Bu}_2\text{Zn}$, it seems plausible that the low yields obtained with ${}^t\text{BuLi}$ are a result of side reactions occurring within this reaction system. Accordingly, the ${}^1\text{H}$ NMR spectrum of $[(\text{PMDETA})\text{Na}(\text{dpa})]$ with ${}^t\text{BuLi}$ was convoluted. Due to the low yields and the lack of *para*-addition observed within our system, this reaction was not studied further. These findings provide a marked contrast to the findings of Yamataka, which revealed that the reaction of ${}^t\text{BuLi}$ with benzophenone in diethyl ether at 0 °C gave carbonyl-addition as the major product (65% yield), alongside a significant quantity of *para*-addition (28% yield).¹⁴



Scheme S1 Reaction of metalloligand **2** with ${}^t\text{BuLi}$ and benzophenone.

4. Neutral zinc complexes containing dpa ligands

As both a soluble and an insoluble product were obtained from the combination of $[(\text{TMEDA})\text{Na}(\text{dpa})]_2$ and R_2Zn , we decided to investigate the reaction chemistry of R_2Zn and $\text{dpa}(\text{H})$ in the absence of the sodium component. Combining R_2Zn with $\text{dpa}(\text{H})$ in a hexane/toluene solvent system at ambient temperature produced a pale yellow solution, from which a crop of colourless crystalline material (yield of 0.08 g, 10 % based on the $\text{dpa}(\text{H})$ stoichiometry, *i.e.*, with a maximum yield of 50 %) was deposited after 24 hours. The molecular structure of these crystals was determined through X-ray crystallography. The identity of the product was revealed to be homoleptic $[\text{Zn}(\text{dpa})_2]$ (**6**), in conflict with the 1:1 stoichiometry of the starting materials. The reaction was successfully repeated on a rational scale, with an isolated crude product yield of 81 %. Unfortunately, the lack of solubility of **6** in C_6D_6 , d_8 -THF, d_5 -pyridine or d_6 -DMSO solvent prevented satisfactory NMR spectroscopic analysis, although resonances corresponding to unreacted $\text{dpa}(\text{H})$ were observed. NMR spectroscopic analysis of the filtrate revealed resonances attributed to dpa anions and R anions, although resonances attributed to more of **6** and to non-coordinated R_2Zn were absent. According to DFT calculations, the synthesis of **6** should be a stable product from the 1:2 combination of ${}^t\text{Bu}_2\text{Zn}$ with $\text{dpa}(\text{H})$, however this product was not observed experimentally and only heteroleptic $[\{(\text{dpa})\text{Zn}({}^t\text{Bu})\}_2]$ was produced. Although **6** is produced from the analogous reaction of R_2Zn with $\text{dpa}(\text{H})$, in a 1:2 stoichiometry, the solid product **6** is contaminated with a significant quantity of the parent amine, $\text{dpa}(\text{H})$. It therefore appears that neither the R_2Zn nor the ${}^t\text{Bu}_2\text{Zn}$ system is capable of generating clean, crystalline **6** in a decent yield.



Scheme S2 Synthesis of homoleptic zinc complex $[\text{Zn}(\text{dpa})_2]$ (**6**).

Turning to the molecular structure of **6**, within it, Zn bonds to four pyridyl N centres in a distorted tetrahedral environment,¹⁵ where the two dpa anions adopt an *anti-anti* conformation (Figure S28). Occupation of the pyridyl pocket by a metal is a common bonding mode, especially for transition metal dipyridylamide complexes (Figure S29).¹⁶⁻¹⁹ Within **6** the four Zn-N bond lengths span a narrow range from 1.9681(17) Å (Zn1-N6) to 1.9851(16) Å (Zn1-N3). These Zn-N bond lengths are marginally shorter than those within the related [Zn{dpa(H)}]²⁺ cation of [Zn{dpa(H)}₂][BF₄]₂ [Zn-N bond lengths of 1.989(3) and 1.990(2) Å], reflecting the switch from anionic dpa to the parent amine, dpa(H).¹⁹ Within **6**, the chelating bond angles of N2-Zn1-N3 and N5-Zn1-N6 are 95.06(7) and 95.88(7)° respectively, similar to the equivalent N-Zn-N bond angle of 95.4(1)° within [Zn{dpa(H)}]²⁺. Examination of the key dipyridylamide bond lengths and angles within **6** suggests that there is a significant degree of resonance delocalisation. Indications of delocalisation include shorter C-N(amido) bonds (typical bond length 1.34 Å), longer C-N(pyridyl) bonds (typical value 1.38 Å) and a near zero dihedral angle between the two pyridyl ring planes.²⁰ Accordingly, the C-N(amido) bond lengths in **6** are short [C1-N1, 1.349(3) Å; C6-N1, 1.349(3) Å; C11-N4, 1.345(3) Å; C16-N4, 1.349(3) Å] and there is a concomitant lengthening of the C-N(pyridyl) bonds [C1-N2, 1.374(2) Å, C6-N3, 1.366(3) Å, C11-N5, 1.371(3) Å, C16-N6, 1.373(2) Å]. The near planarity of the two pyridyl ring planes provides further evidence for resonance delocalisation of the anionic charge (the dihedral angle is 1.702° between the C1...N2 and the C6...N3 ring planes, and is 3.327° between the C16...N6 and the C11...N5 ring planes). Similar to those in previously reported structures,²¹ there are two long C-N bonds, two shorter C-C bonds and two longer C-C bonds within each pyridyl ring, indicative of a N-C-C=C-C=C-N substitution pattern [bond lengths 1.374(2)/1.359(3), 1.428(3)/1.429(3), 1.361(3)/1.363(3), 1.405(3)/1.400(3), 1.366(3)/1.358(3), 1.363(3)/1.359(3)]. With a dihedral angle of 88.137°, the two dpa units are practically perpendicular to each other.

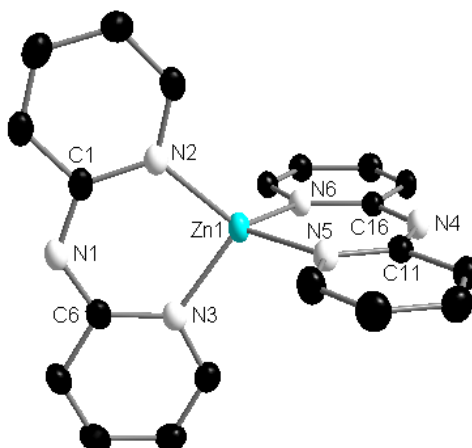


Figure S28 Molecular structure of **6** with thermal ellipsoids at 50% probability level and hydrogen atoms omitted for clarity. Selected bond lengths (Å) and angles (°): Zn1-N2, 1.9698(16); Zn1-N3, 1.9851(16); Zn1-N5, 1.9773(16); Zn1-N6, 1.9681(17); N1-C1, 1.349(3); N1-C6, 1.349(3); N2-C1, 1.374(2); N3-C6, 1.366(3); N4-C11, 1.345(3); N4-C16, 1.349(3); N5-C11, 1.371(3); N6-C16, 1.373(2); N2-C1, 1.374(2); C1-C2, 1.428(3); C2-C3, 1.361(3); C3-C4, 1.405(3); C4-C5, 1.366(3); N2-C5, 1.363(3); N3-C6, 1.359(3); C6-C7, 1.429(3); C7-C8, 1.363(3); C8-C9, 1.400(3); C9-C10, 1.358(3); N3-C10, 1.359(3); N2-Zn1-N3, 95.06(7); N2-Zn1-N5, 119.20(7); N2-Zn1-N6, 123.01(6); N3-Zn1-N5, 108.72(7); N3-Zn1-N6, 115.57(6); N5-Zn1-N6, 95.88(7); C1-N1-C6, 127.92(16); C11-N4-C16, 128.59(17), N1-C1-N2, 126.89(17); N1-C6-N3, 125.93(17); N4-C11-N5, 125.94(18); N4-C16-N6, 126.52(17).

Isostructural to **6**, the most relevant comparison is probably the neutral cobalt (II) complex $[\text{Co}(\text{dpa})_2]$ (Figure S29), which was prepared through a salt metathesis reaction combining Lidpa with CoCl_2 .¹⁶ However, possibly the most interesting comparison for **6** is provided by the substituted dpa, neutral zinc species $[\text{Zn}(\text{dpa}^*)_2]$ [where dpa* is 6,6'-di-*tert*-butyl(dpa)].²² Within this alkyl-substituted variant of **6**, both dpa* ligands adopt a *syn-anti* conformation and the pyridyl pocket is not occupied by Zn, contrasting with the *anti-anti* dpa conformation within **6**. This difference is clearly an artefact of the increased steric demands of the bulky *tert*-butyl substituents of dpa*. Looking at the molecular structure, the pyridine rings of $[\text{Zn}(\text{dpa}^*)_2]$ are not equivalent, however only one set of pyridyl NMR resonances is observed in C_6D_6 solution. This suggests that the pyridyl rings interconvert too rapidly to observe two distinct sets of resonances on the NMR timescale due to a low rotational barrier.

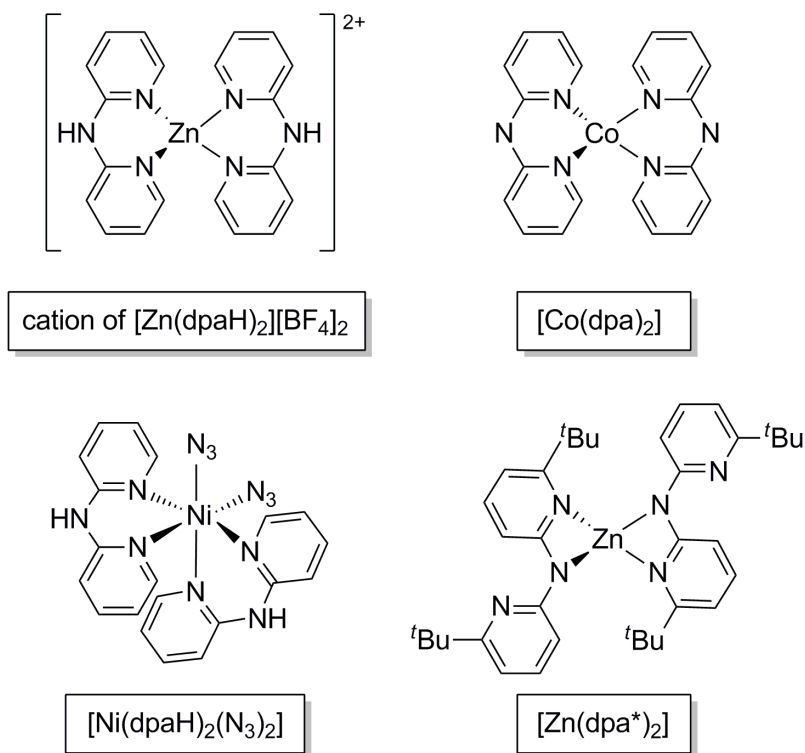


Figure S29 Graphical representation of transition metal neutral dipyridylamine and anionic dipyridylamide complexes.

DFT calculations were performed to probe the relative energies of the regioisomers of $[\text{Zn}(\text{dpa})_2]$ based upon different *anti-anti* (models **6_{calc-A}** and **6_{calc-B}**), *syn-syn*, (model **6_{calc-C}**) and *syn-anti* (models **6_{calc-D}** and **6_{calc-E}**) conformations of the dpa ligand (Figure S30), using the Gaussian computational package G03.²³ In this series of calculations the B3LYP^{24, 25} density functionals and the 6-311G(d,p)^{26, 27} basis set were used. These computations reinforced that model **6_{calc-A}**, having the experimentally observed structure, is the most thermodynamically favourable isomer. A comparison of the geometrical parameters calculated for model **6_{calc-A}** with those obtained experimentally through X-ray determination of the solid state structures show good agreement. The next energy minimum structure is that of **6_{calc-D}**, by +10.69 kcal mol⁻¹, which closely resembles the structure of crystalline $[\text{Zn}(\text{dpa}^*)_2]$. With an *anti-anti* dpa conformation, **6_{calc-B}** is the most high energy structure (+53.53 kcal mol⁻¹) due to the low coordination of Zn (two-coordinate). The charge density distribution within **6_{calc-A}** reveals that the charge density couples into

the formally neutral pyridyl rings, as the pyridyl N atoms (natural charge of -0.76) carry more negative charge than the bridging, amido N (natural charge of -0.63).

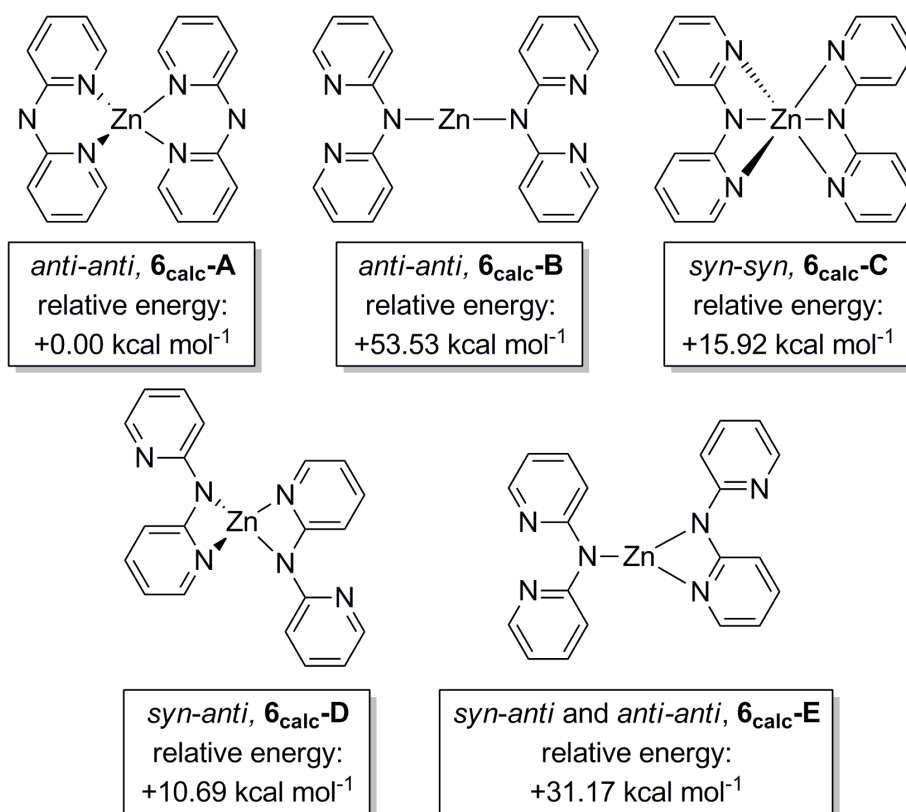


Figure S30 Relative energies of DFT-modelled compounds **6_{calc}-A-E**.

5. DFT Calculations

DFT calculations were performed using the Gaussian computational package G03.²³ In this series of calculations the B3LYP^{24, 25} density functionals and the 6-311G(d,p)^{26, 27} basis set were used. After each geometry optimisation, a frequency analysis was performed and the energy values quoted include the zero point energy contribution.

5.1 [(PMDETA)Na(dpa)]₂, **2**_{calc}

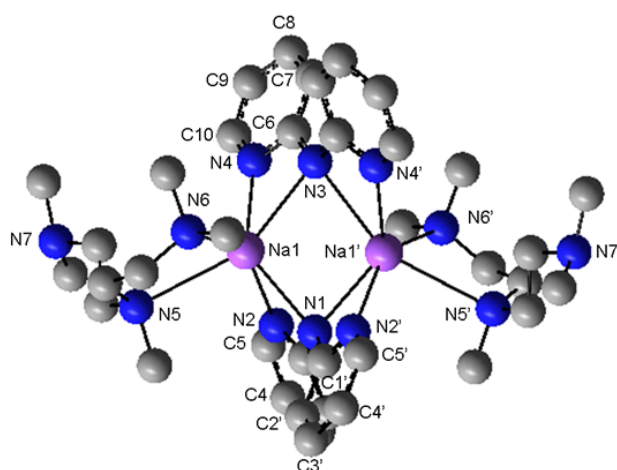
In view of the problems with the crystal structure of **2** we employed a DFT (density functional theory) study to model the molecular structure of **2**. The resultant optimised geometries were subjected to a frequency analysis, and the total energy computed by the DFT calculation was adjusted by inclusion of the zero-point energy contribution.

The xyz coordinates determined from the crystal structure of **2** were taken as the starting point for model **2**_{calc}, with subsequent optimisation of the geometry. Significantly the key feature of experimental **2** is replicated in model **2**_{calc}, as only two of the three PMDETA N atoms engage the Na atom. Within dimeric **2**_{calc}, a C₂ axis of symmetry runs through N1 and N3. Thus each *syn-syn* dpa unit forms a symmetrical bridge between the two Na centres, although there are slight differences in their coordination towards Na. The first dpa unit displays similar (amido)N-Na and (pyridyl)N-Na bond lengths (Na1-N1, 2.541 Å and Na1-N2, 2.511 Å, respectively). In contrast, Na draws considerably closer to the terminal, (pyridyl)N arm (Na1-N4, 2.451 Å) of the second dpa fragment than it does to the (amido)N centre (Na1-N3, 2.704 Å). Inspection of the bond lengths of **2**_{calc} reveals that resonance delocalisation of the anionic charge occurs within both dpa units. In comparison to bond length data from related neutral dpa(H) and anionic dpa complexes, the (amido)N-C bond lengths of **2**_{calc} are short (N1-C1, 1.363 Å; N3-C6, 1.362 Å), whilst the (pyridyl)N-C bonds of **2**_{calc} are elongated due to the loss of aromaticity (N2-C1, 1.364 Å; N4-C6, 1.365 Å).²⁷⁻³⁰ This contrasts with the bonding pattern observed within the neutral

dpa(H) cobalt species $[\text{Co}\{\text{dpa}(\text{H})\}\text{Cl}_2]$, where the (amine)N-C bond lengths are long [1.373(4) and 1.382(4) Å] in comparison to the (pyridyl)N-C bonds [1.351(4) and 1.348(4) Å].¹⁶

Principal Bond Lengths (Å)

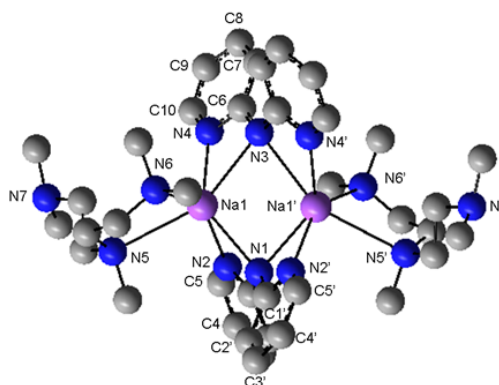
Na1-N1	2.541	N1-C1	1.363
Na1-N2	2.511	N2-C1	1.364
Na1-N3	2.704	N2-C5	1.335
Na1-N4	2.451	C1-C2	1.424
Na1-N5	2.877	C2-C3	1.382
Na1-N6	2.612	C3-C4	1.399
		C4-C5	1.389



N3-C6	1.362
N4-C6	1.365
N4-C10	1.337
C6-C7	1.426
C7-C8	1.380
C8-C9	1.400
C9-C10	1.387

Principal Bond Angles (°)

N1-Na1-N2	54.0
N3-Na1-N4	52.9
N5-Na1-N6	67.8
N1-Na1-N3	98.9
Na1-N1-Na1'	84.0
Na1-N3-Na1'	77.9

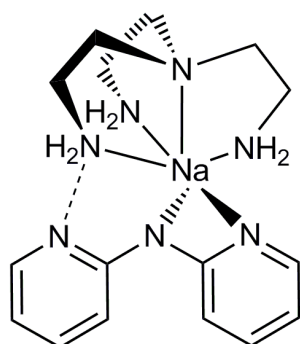


5.2 [(H₆-TREN)Na(dpa)], 4_{calc}5.2.1 Total Energies (a.u.) and Relative Energies (kcal mol⁻¹)

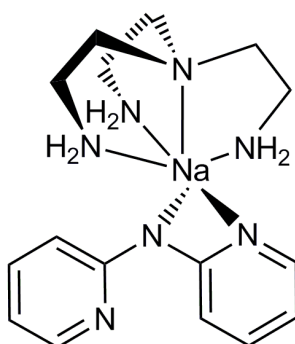
Model 4_{calc}-A	-1170.840325	0.00
---------------------------------	---------------------	-------------

Model 4_{calc}-B	-1170.835238	+3.19
---------------------------------	---------------------	--------------

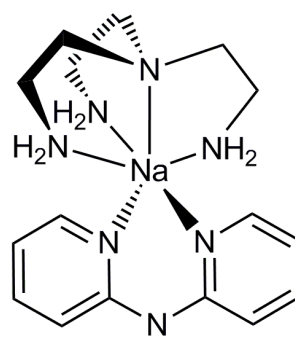
Model 4_{calc}-C	-1170.825977	+9.00
---------------------------------	---------------------	--------------



syn-syn, 4_{calc}-A
relative energy:
0.00 kcal mol⁻¹



syn-anti, 4_{calc}-B
relative energy:
+3.19 kcal mol⁻¹



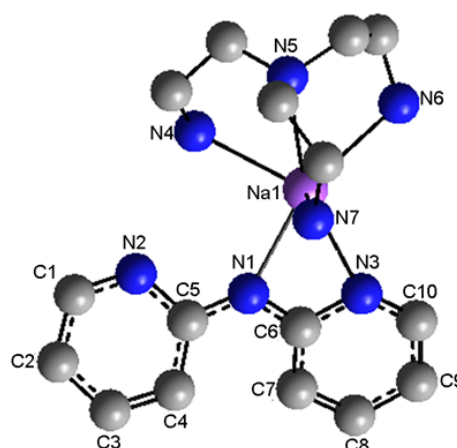
anti-anti, 4_{calc}-C
relative energy:
+9.00 kcal mol⁻¹

5.2.2 4_{calc}-A (*syn-syn*)

Principal Bond Lengths (Å)

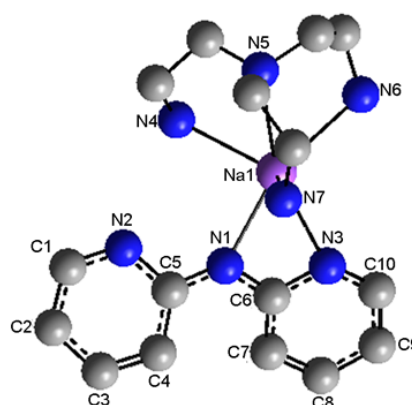
N1-C5	1.353	N1-C6	1.351
N2-C5	1.368	N3-C6	1.373
N2-C1	1.334	N3-C10	1.333
C1-C2	1.389	C9-C10	1.389
C2-C3	1.399	C8-C9	1.400
C3-C4	1.381	C7-C8	1.380
C4-C5	1.427	C6-C7	1.428

Na1-N1	2.388
Na1...N2	3.720
Na1-N3	2.539
Na1-N6	2.526
Na1-N7	2.510
Na1-N4	2.516
Na1-N5	2.756
C5-N1-C6	126.2
(N4)H...N2	2.068
N2...N4	3.071



Principal Bond Angles (°)

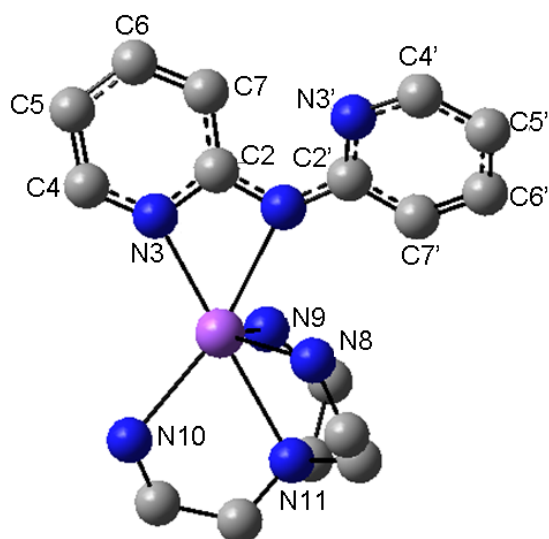
N1-Na1-N3	55.1
N1-Na1-N4	86.3
N1-Na1-N5	138.8
N1-Na1-N6	151.6
N1-Na1-N7	91.9
N3-Na1-N4	131.1
N3-Na1-N5	159.2
N3-Na1-N6	99.1
N3-Na1-N7	99.5
N4-Na1-N5	69.7
N4-Na1-N6	107.2
N4-Na1-N7	111.8
N5-Na1-N6	69.5
N5-Na1-N7	68.4
N6-Na1-N7	105.3



5.2.3 4_{calc}-B (*syn-anti*)

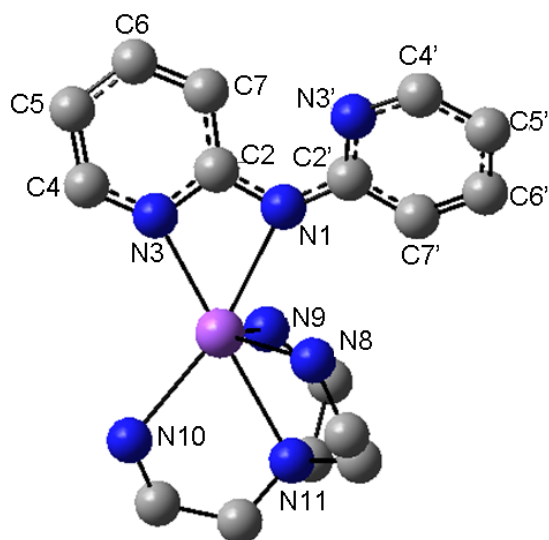
Principal Bond Lengths (Å)

		′
N1-C2	1.367	1.360
C2-N3	1.368	1.360
N3-C4	1.337	1.333
C4-C5	1.385	1.390
C5-C6	1.401	1.400
C6-C7	1.379	1.380
C7-C2	1.424	1.430
Na-N1	2.522	
Na-N3	2.397	
Na-N8	2.513	
Na-N9	2.508	
Na-N10	2.521	
Na-N11	2.664	



Principal Bond Angles (°)

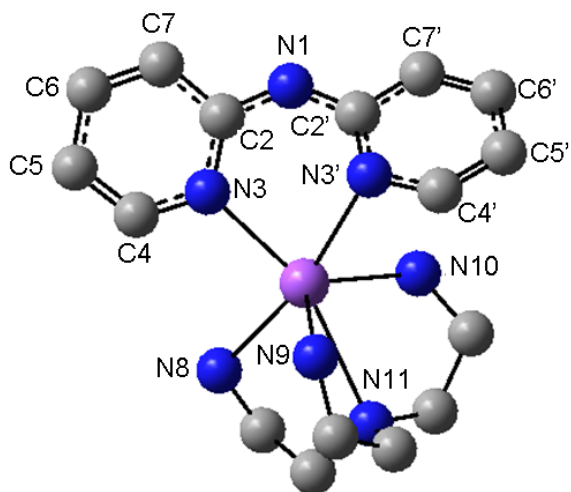
C2-N1-C2′	123.6
N1-Na-N3	55.5
N8-Na-N9	118.0
N8-Na-N10	101.3
N8-Na-N11	70.2
N9-Na-N10	126.3
N9-Na-N11	71.1
N10-Na-N11	71.4
C2′-N1-C2-C3	-159.1



5.2.4 4_{calc}-C (*anti-anti*)

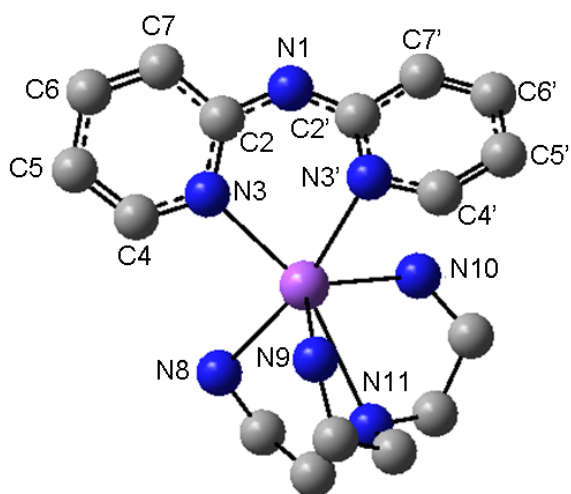
Principal Bond Lengths (Å)

		Å
N1-C2	1.350	1.334
C2-N3	1.366	1.377
N3-C4	1.342	1.340
C4-C5	1.383	1.385
C5-C6	1.405	1.411
C6-C7	1.374	1.372
C7-C2	1.430	1.440
Na-N3	2.378	2.498
Na-N8	2.573	
Na-N9	2.508	
Na-N10	2.564	
Na-N11	2.791	



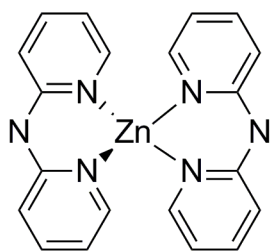
Principal Bond Angles (°)

C2-N1-C2'	128.2
N3-Na-N3'	76.9
N8-Na-N9	100.8
N8-Na-N10	100.2
N8-Na-N11	67.9
N9-Na-N10	119.5
N9-Na-N11	68.6
N10-Na-N11	68.4

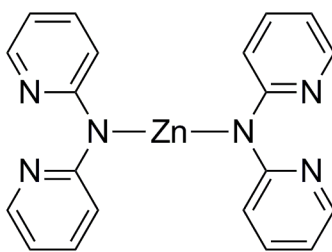


5.3 [Zn(dpa)₂], **6_{calc}**5.3.1 Total Energies (a.u.) and Relative Energies (kcal mol⁻¹)

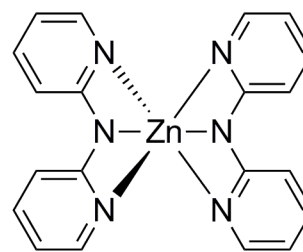
Model 6_{calc}-A	-2879.626561	0.00
Model 6_{calc}-B	-2879.541277	+53.53
Model 6_{calc}-C	-2879.601186	+15.92
Model 6_{calc}-D	-2879.609525	+10.69
Model 6_{calc}-E	-2879.576896	+31.17



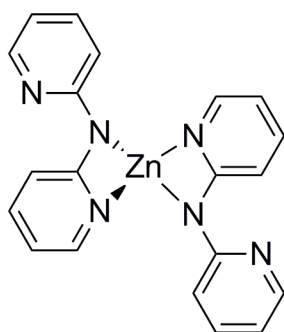
anti-anti, **6_{calc}-A**
relative energy:
+0.00 kcal mol⁻¹



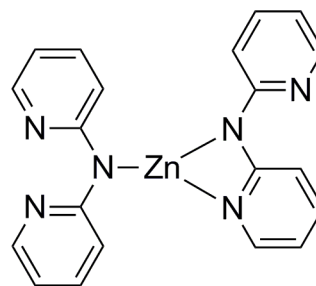
anti-anti, **6_{calc}-B**
relative energy:
+53.53 kcal mol⁻¹



syn-syn, **6_{calc}-C**
relative energy:
+15.92 kcal mol⁻¹



syn-anti, **6_{calc}-D**
relative energy:
+10.69 kcal mol⁻¹

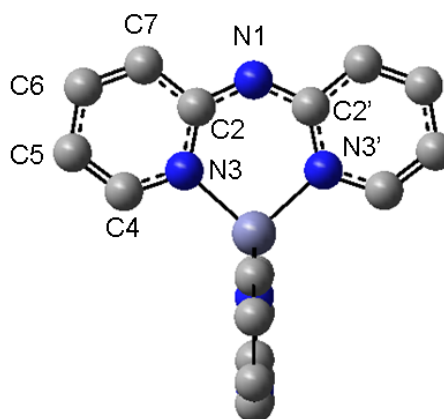


syn-anti and anti-anti, **6_{calc}-E**
relative energy:
+31.17 kcal mol⁻¹

5.3.2 [Zn(dpa)₂], 6_{calc}-A

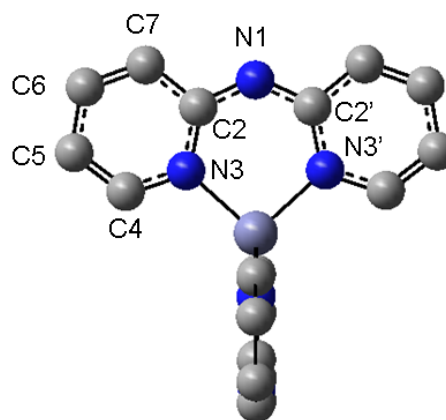
Principal Bond Lengths (Å) and Bond Angles (°)

N1-C2	1.340
C2-N3	1.377
N3-C4	1.357
C4-C5	1.372
C5-C6	1.411
C6-C7	1.369
C7-C2	1.431
Zn-N3	2.736
C2-N1-C2'	129.8
Zn-N3-C2	121.0
N3-Zn-N3'	95.7
C2'-N1-C2-N3	0.0



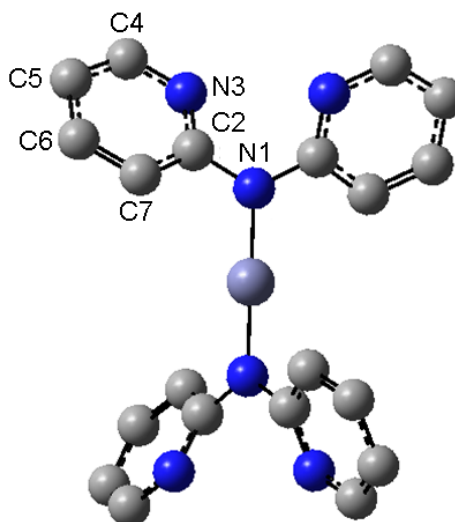
Natural Charges and Bond Indices

N1	-0.63	N1-C2	1.32
C2	+0.42	C2-N3	1.22
N3	-0.76	N3-C4	1.30
C4	+0.08	C4-C5	1.53
C5	-0.29	C5-C6	1.30
C6	-0.16	C6-C7	1.57
C7	-0.22	C7-C2	1.23
Zn	+1.70	Zn-N3	0.15



5.3.3 [Zn(dpa)₂], 6_{calc}-B**Principal Bond Lengths (Å) and Bond Angles (°)**

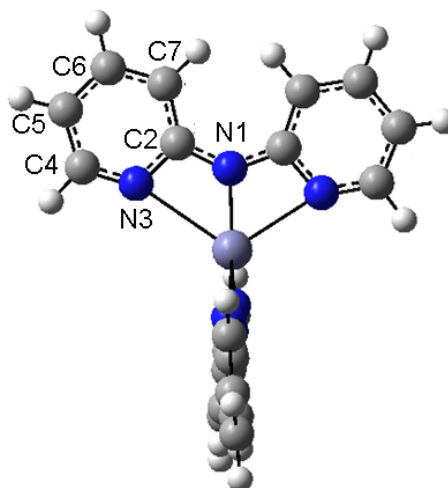
N1-C2	1.402
C2-N3	1.336
N3-C4	1.333
C4-C5	1.392
C5-C6	1.393
C6-C7	1.386
C7-C2	1.408
Zn-N	1.835
C2-N1-C2'	121.8
Zn-N1-C2	119.1
N1-Zn-N1	180.0
C2'-N1-C2-N3	32.7



5.3.4 [Zn(dpa)₂], 6_{calc}-C

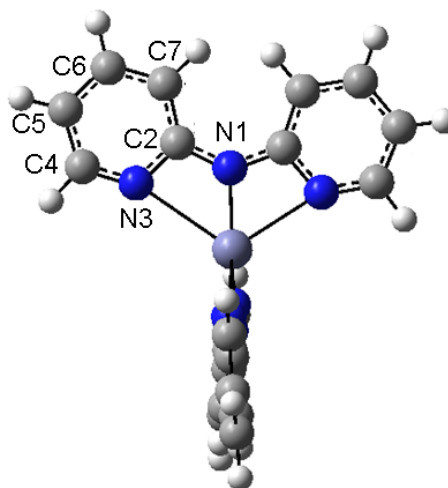
Principal Bond Lengths (Å)

N1-C2	1.369	1.366
C2-N3	1.358	1.363
N3-C4	1.330	1.330
C4-C5	1.392	1.391
C5-C6	1.393	1.394
C6-C7	1.387	1.387
C7-C2	1.410	1.410
Zn-N1	1.900	
Zn-N3	2.736	2.494



Principal Bond Angles (°)

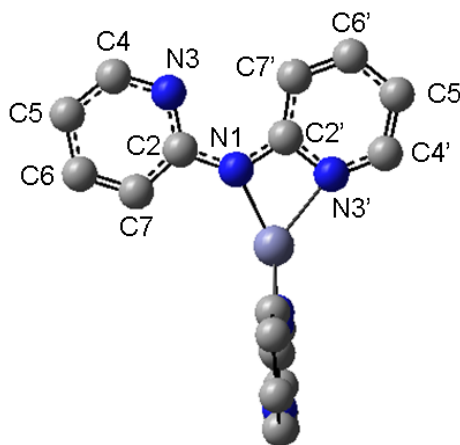
C2-N1-C2'	134.4	
Zn-N1-C2	116.6	109.0
N1-Zn-N1'	176.5	
N3-Zn-N3'	113.5	
N1-Zn-N3'	54.3	59.2
C2'-N1-C2-N3	-176.1	-175.9



5.3.5 [Zn(dpa)₂], 6_{calc}-D

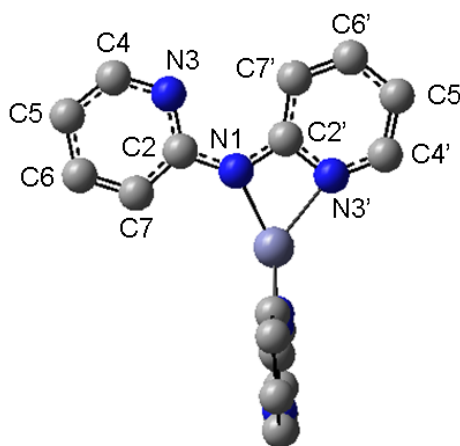
Principal Bond Lengths (Å)

N1-C2	1.377	1.365
C2-N3	1.344	1.370
N3-C4	1.338	1.336
C4-C5	1.387	1.385
C5-C6	1.399	1.401
C6-C7	1.380	1.383
C7-C2	1.415	1.412
Zn-N1	1.975	
Zn-N3	2.122	



Principal Bond Angles (°)

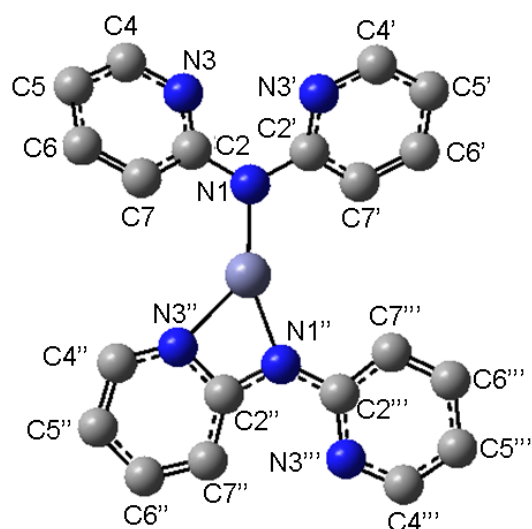
C2-N1-C2'	127.8	
Zn-N1-C2	136.2	96.0
N1-Zn-N1	143.2	
N3-Zn-N3	121.0	
N1-Zn-N3'	65.7	
C2'-N1-C2-N3	1.2	-179.9



5.3.6 [Zn(dpa)₂], 6_{calc}-E

Principal Bond Lengths (Å)

		'	''	'''
N1-C2	1.397	1.396	1.368	1.382
C2-N3	1.339	1.339	1.370	1.341
N3-C4	1.333	1.332	1.337	1.338
C4-C5	1.392	1.392	1.384	1.387
C5-C6	1.394	1.394	1.401	1.398
C6-C7	1.386	1.386	1.384	1.381
C7-C2	1.410	1.411	1.410	1.414
Zn-N1	1.862		1.950	
Zn-N3			2.102	



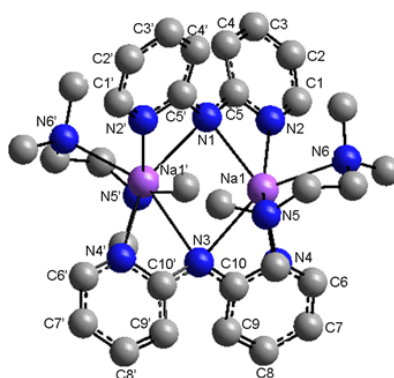
Principal Bond Angles (°)

		'	''	'''
C2-N1-C2'	121.4		127.8	
Zn-N1-C2	119.7	118.7	95.9	136.3
N1-Zn-N1	157.6			
N1-Zn-N3	66.4			
C2'-N1-C2-N3	33.6	32.5	2.7	-177.2

5.4 [(TMEDA)Na(dpa)]₂, δ_{calc}

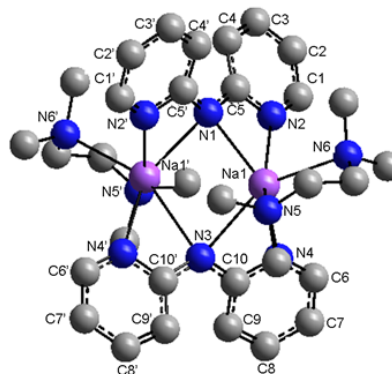
Principal Bond Lengths (Å)

N1-C5	1.363	Na1-N1	2.520
C5-N2	1.363	Na1-N2	2.556
N2-C1	1.335	Na1-N3	2.700
C1-C2	1.389	Na1-N4	2.425
C2-C3	1.400	Na1-N5	2.638
C3-C4	1.381	Na1-N6	2.659
C4-C5	1.424		
N3-C10	1.361		
C10-N4	1.365		
N4-C6	1.336		
C6-C7	1.387		
C7-C8	1.400		
C8-C9	1.380		
C9-C10	1.426		



Principal Bond Angles (°)

C5-N1-C5'	123.7
C10-N3-C10'	122.6
N1-Na1-N2	53.7
N5-Na1-N6	70.4
N3-Na1-N4	53.1
N1-Na1-N3	100.1
Na1-N1-Na1'	83.3
Na1-N1-Na1'	76.6



6. Discussion of Dpa Bond Lengths and Bond Angles

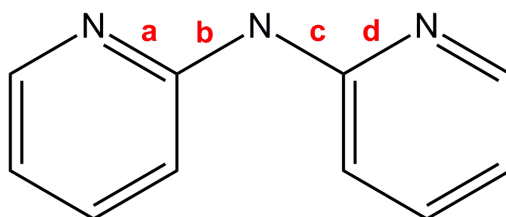


Table S7 Key bond lengths for a range of neutral and anionic dpa complexes.

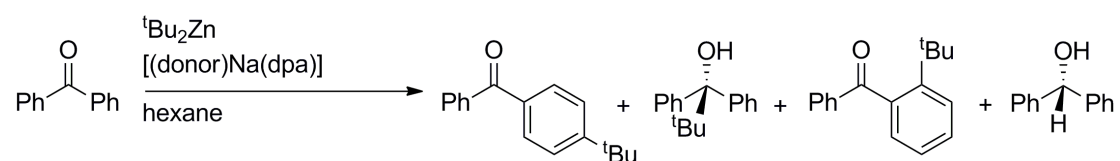
Compound		Bond Length (Å)			
		a	b	c	D
dpa(H) monoclinic ²⁸		1.343(2)	1.388(2)	1.391(2)	1.335(2)
dpa(H) orthorhombic ²⁹		1.332(4)	1.379(4)	1.380(4)	1.338(4)
dpa(H) triclinic ³⁰		1.337(2)	1.380(3)	1.376(3)	1.334(3)
[Co{dpa(H)}Cl ₂] ¹⁶		1.351(4)	1.373(4)	1.382(4)	1.348(4)
[Co(dpa) ₂] ¹⁶		1.367(4)	1.346(4)	1.344(4)	1.371(4)

7. Tables of Results

7.1 Donor Ligand Variation

Variation of donor ligands: stoichiometric conditions

ⁿBuNa (0.16 g, 2 mmol) was suspended in hexane (6 mL) and dpa(H) (0.34g, 2 mmol) was added. The resultant beige suspension was allowed to stir for 45 minutes at ambient temperature. To this, the donor ligand was injected [DMAP (0.24 g, 2 mmol); TEMPO (0.31 g 2 mmol); TMEDA (0.30 mL, 2 mmol); PMDETA (0.42 mL, 2 mmol); TMDAE (0.38 mL, 2 mmol); H₆-TREN (0.30 mL, 2 mmol); Me₆-TREN (0.42 mL, 2 mmol)]. A hexane solution of ^tBu₂Zn (2 mL of a 0.5 M solution, 1 mmol) was subsequently added, followed by benzophenone (0.18 g, 1 mmol) and the reaction was stirred for 18 h, either at ambient temperature or at 75°C prior to work-up.



Scheme S3 General reaction scheme for the metalloligand assisted *tert*-butylation of benzophenone with variation of the Lewis donor.

Variation of donor ligands: catalytic conditions

ⁿBuNa (0.08 g, 1 mmol) was suspended in hexane (30 mL) and dpa(H) (0.17 mL, 1 mmol) was added. The reaction mixture was allowed to stir for 45 minutes. Subsequently, the donor ligand was added [DMAP (0.12 g, 1 mmol); TMEDA (0.15 mL, 1 mmol); PMDETA (0.21 mL, 1 mmol); TMDAE (0.14 mL, 1 mmol)]. Following this, ^tBu₂Zn (10 mL of a 0.5 M solution of ^tBu₂Zn in hexane, 5 mmol), and benzophenone (0.90 g, 5 mmol) were added. The reaction mixture was stirred under reflux conditions for 18 h, prior to work-up.

7.1.1 Reactions with [(DMAP)Na(dpa)]

Stoichiometric reaction conditions, ambient temperature, 18 hours:

Ligand	Solvent	1,2 Addition (%)	1,4 Addition (%)	1,6 Addition (%)	Benzhydrol (%)	Total Yield (%)
DMAP	Hexane	8	0	21	7	36
DMAP	Hexane	3	0	27	2	32

Stoichiometric reaction conditions, 75°C, 18 hours:

Ligand	Solvent	1,2 Addition (%)	1,4 Addition (%)	1,6 Addition (%)	Benzhydrol (%)	Total Yield (%)
DMAP	Hexane	13	0	26	6	45
DMAP	Hexane	15	0	24	9	48

Catalytic reaction conditions, 75°C, 18 hours:

Ligand	Solvent	1,2 Addition (%)	1,4 Addition (%)	1,6 Addition (%)	Benzhydrol (%)	Total Yield (%)
DMAP	Hexane	9	0	30	6	45
DMAP	Hexane	7	0	21	7	35

7.1.2 Reactions with [(TMEDA)Na(dpa)]₂²⁰

Stoichiometric reaction conditions, 75°C, 18 hours:

Ligand	Solvent	1,2 Addition (%)	1,4 Addition (%)	1,6 Addition (%)	Benzhydrol (%)	Total Yield (%)
TMEDA	Hexane	9	2	43	13	67
TMEDA	Hexane	8	2	36	25	71
TMEDA	Hexane	12	1	43	14	69
TMEDA	Hexane	16	3	54	5	78

7.1.3 Reactions with [(TMDAE)Na(dpa)]₂

Stoichiometric reaction conditions, ambient temperature, 18 hours:

Ligand	Solvent	1,2 Addition (%)	1,4 Addition (%)	1,6 Addition (%)	Benzhydrol (%)	Total Yield (%)
TMDAE	Hexane	1	0	2	0	3
TMDAE	Hexane	1	0	3	0	4
TMDAE	Hexane	1	0	2	0	3

Stoichiometric reaction conditions, 75°C, 18 hours:

Ligand	Solvent	1,2 Addition (%)	1,4 Addition (%)	1,6 Addition (%)	Benzhydrol (%)	Total Yield (%)
TMDAE	Hexane	9	2	46	3	60
TMDAE	Hexane	9	0	43	3	55

Catalytic reaction conditions, 75°C, 18 hours:

Ligand	Solvent	1,2 Addition (%)	1,4 Addition (%)	1,6 Addition (%)	Benzhydrol (%)	Total Yield (%)
TMDAE	Hexane	6	0	24	3	33
TMDAE	Hexane	7	0	26	3	36

7.1.4 Reactions with [(PMDETA)Na(dpa)]₂

Stoichiometric reaction conditions, ambient temperature, 18 hours:

Ligand	Solvent	1,2 Addition (%)	1,4 Addition (%)	1,6 Addition (%)	Benzhydrol (%)	Total Yield (%)
PMDETA	Hexane	2	1	41	16	60
PMDETA	Hexane	3	0	46	7	56
PMDETA	Hexane	2	1	43	10	56

Stoichiometric reaction conditions, 75°C, 18 hours:

Ligand	Solvent	1,2 Addition (%)	1,4 Addition (%)	1,6 Addition (%)	Benzhydrol (%)	Total Yield (%)
PMDETA	Hexane	3	1	44	20	68
PMDETA	Hexane	2	1	51	1	55
PMDETA	Hexane	5	0	44	8	57

Catalytic reaction conditions, 75°C, 18 hours:

Ligand	Solvent	1,2 Addition (%)	1,4 Addition (%)	1,6 Addition (%)	Benzhydrol (%)	Total Yield (%)
PMDETA	Hexane	5	0	54	7	66
PMDETA	Hexane	6	0	58	6	70
PMDETA	Hexane	5	0	53	4	62
PMDETA	Hexane	9	0	47	7	63

7.1.5 Reactions with [(H₆-TREN)Na(dpa)]

Stoichiometric reaction conditions, ambient temperature, 18 hours:

Ligand	Solvent	1,2 Addition (%)	1,4 Addition (%)	1,6 Addition (%)	Benzhydrol (%)	Total Yield (%)
H ₆ TREN	Hexane	1	0	1	1	3
H ₆ TREN	Hexane	2	0	1	6	9

Stoichiometric reaction conditions, 75°C, 18 hours:

Ligand	Solvent	1,2 Addition (%)	1,4 Addition (%)	1,6 Addition (%)	Benzhydrol (%)	Total Yield (%)
H ₆ TREN	Hexane	5	0	6	7	18
H ₆ TREN	Hexane	3	0	4	6	13

7.1.6 Reactions with [(Me₆-TREN)Na(dpa)]

Stoichiometric reaction conditions, ambient temperature, 18 hours:

Ligand	Solvent	1,2 Addition (%)	1,4 Addition (%)	1,6 Addition (%)	Benzhydrol (%)	Total Yield (%)
Me ₆ TREN	Hexane	1	0	1	1	3
Me ₆ TREN	Hexane	0	0	0	0	0

Stoichiometric reaction conditions, 75°C, 18 hours:

Ligand	Solvent	1,2 Addition (%)	1,4 Addition (%)	1,6 Addition (%)	Benzhydrol (%)	Total Yield (%)
Me ₆ TREN	Hexane	12	0	26	9	45
Me ₆ TREN	Hexane	13	0	32	15	60
Me ₆ TREN	Hexane	13	0	37	6	56
Me ₆ TREN	Hexane	15	0	41	15	71

7.1.7 Reaction with [(TEMPO)Na(dpa)]

Stoichiometric reaction conditions, ambient temperature, 18 hours:

Ligand	Solvent	1,2 Addition (%)	1,4 Addition (%)	1,6 Addition (%)	Benzhydrol (%)	Total Yield (%)
TEMPO	Hexane	0	0	0	0	0
TEMPO	Hexane	0	0	0	2	2

7.1.8 Reaction with [(PMDETA)Na(dpa)]₂ and TEMPO

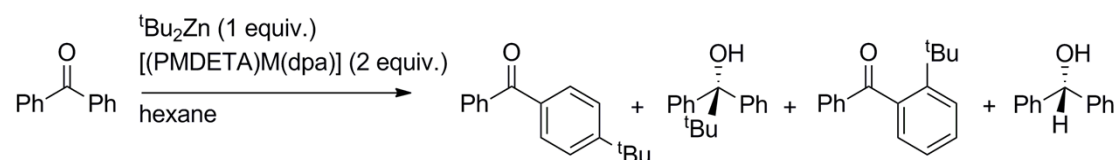
Dpa(H) (0.34 g, 2 mmol) was added to a freshly prepared suspension of BuNa (0.16 g, 2 mmol) in hexane (8 mL) and the reaction mixture was stirred for 45 minutes at ambient temperature. Subsequently, PMDETA (0.42 mL, 2 mmol), TEMPO (0.31 g, 2 mmol), ^tBu₂Zn (2 mL of a 0.5 M solution in hexane, 1 mmol) and benzophenone (0.18 g, 1 mmol) were added and the reaction mixture was stirred at ambient temperature for 18 hours prior to work-up.

Stoichiometric reaction conditions, ambient temperature, 18 hours:

Ligand	Solvent	1,2 Addition (%)	1,4 Addition (%)	1,6 Addition (%)	Benzhydrol (%)	Total Yield (%)
PMDETA/TEMPO	Hexane	0	0	0	0	0
PMDETA/TEMPO	Hexane	0	0	1	1	0
PMDETA/TEMPO	Hexane	0	0	3	2	5

7.2 Variation of the Alkali Metal

Variation of alkali metal: reaction with Lidpa, Nadpa or Kdpa



Scheme S4 General reaction scheme for the metalloligand assisted *tert*-butylation of benzophenone with variation of the alkali metal, M = Li, Na, K.

Following the introduction of an organometallic reagent R'M [R'M = BuLi (1.25 mL, 1.6 M in hexanes solution, 2 mmol); ⁿBuNa (0.16 g, 2 mmol); or KR (0.25 g, 2 mmol) (where R is CH₂SiMe₃)] to hexanes solvent (6 mL), dpa(H) (0.34 g, 2 mmol) was added *via* a solid addition tube. The resultant beige suspension was then stirred for 45 minutes at ambient temperature. To this, PMDETA was injected (0.42 mL, 2 mmol), followed by a hexane solution of ^tBu₂Zn (2 mL of a 0.5 M solution, 1 mmol). Benzophenone (0.18 g, 1 mmol) was subsequently added and the reaction was stirred for 18 hours at ambient temperature prior to work-up.

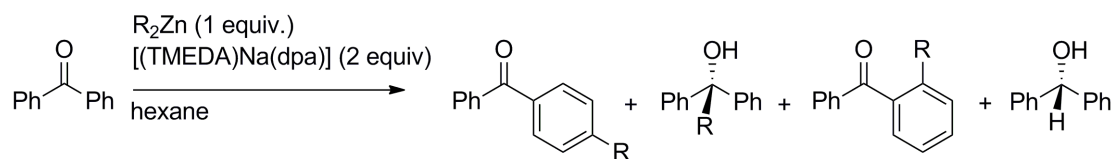
Lidpa, stoichiometric conditions, room temperature, 18 hours:

Ligand	Solvent	1,2 Addition (%)	1,4 Addition (%)	1,6 Addition (%)	Benzhydrol (%)	Total Yield (%)
PMDETA	Hexane	20	0	23	19	62
PMDETA	Hexane	17	0	19	16	52

Kdpa, stoichiometric conditions, room temperature, 18 hours:

Ligand	Solvent	1,2 Addition (%)	1,4 Addition (%)	1,6 Addition (%)	Benzhydrol (%)	Total Yield (%)
PMDETA	Hexane	2	0	2	0	4
PMDETA	Hexane	1	0	2	0	3

7.3 Variation of the R Group: Reaction with $\text{Zn}(\text{CH}_2\text{Si}(\text{CH}_3)_3)$



Scheme S5 General reaction scheme for the metalloligand assisted alkylation of benzophenone with ZnR_2 [R is $(\text{CH}_2)\text{SiMe}_3$].

$n\text{BuNa}$ (0.16 g, 2 mmol) was suspended in hexane (6 mL) and $\text{dpa}(\text{H})$ (0.34g, 2 mmol) was added. After the reaction mixture was stirred for 1 h, TMEDA (0.30 mL, 2 mmol) was added, followed by R_2Zn (2 mL of a 0.5 M solution in hexane, 1 mmol). Following the addition of benzophenone (0.18 g, 1 mmol), the reaction was allowed to stir for 18 h, either at ambient temperature or under reflux conditions prior to work-up.

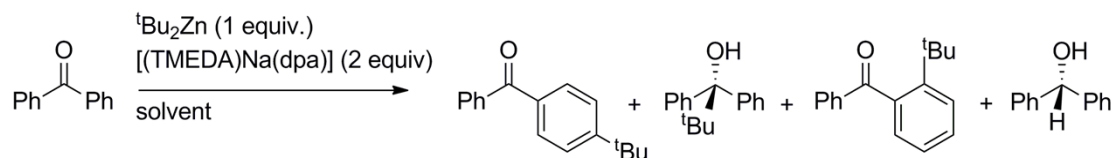
Stoichiometric reaction conditions, ambient temperature, 18 hours:

Ligand	Solvent	1,2 Addition (%)	1,4 Addition (%)	1,6 Addition (%)	Benzhydrol (%)	Total Yield (%)
TMEDA	Hexane	0	0	0	0	0
TMEDA	Hexane	0	0	0	0	0

Stoichiometric reaction conditions, 75°C, 18 hours:

Ligand	Solvent	1,2 Addition (%)	1,4 Addition (%)	1,6 Addition (%)	Benzhydrol (%)	Total Yield (%)
TMEDA	Hexane	0	0	0	7	7
TMEDA	Hexane	0	0	0	8	8

7.4 Variation of the Solvent System



Scheme S6 General reaction scheme for the metalloligand assisted *tert*-butylation of benzophenone with variation of the bulk solvent.

ⁿBuNa (0.16 g, 2 mmol) was suspended in hexane (6 mL) and dpa(H) (0.34 g, 2 mmol) was added. The resultant beige suspension was allowed to stir for 45 minutes at ambient temperature, following which, all solvent was removed *in vacuo*. THF (6 mL), TMEDA (0.30 mL, 2 mmol), and ^tBu₂Zn (2 mL of a 0.5 M solution in THF, 1 mmol) were then added.^[a] Following the addition of benzophenone (0.18 g, 1 mmol), the reaction was allowed to stir at ambient temperature for 18 h, over which time a colour change from orange to green was observed. The reaction was worked up as per Method A.

[a] When the reaction was performed in a mixed THF/hexane solvent system, hexane (4 mL), TMEDA (0.30 mL, 2 mmol), THF (2 mL) and ^tBu₂Zn (2 mL of a 0.5 M solution in THF, 1 mmol) were injected.

Stoichiometric reaction conditions, ambient temperature, hexane solvent, 18 hours: see Section 7.1.2.

Stoichiometric reaction conditions, ambient temperature, hexane/THF solvent system, 18 hours:

Ligand	Solvent	1,2 Addition (%)	1,4 Addition (%)	1,6 Addition (%)	Benzhydrol (%)	Total Yield (%)
TMEDA	Hexane/THF	4	0	11	2	17
TMEDA	Hexane/THF	3	0	5	1	9
TMEDA	Hexane/THF	2	0	6	1	9

Stoichiometric reaction conditions, ambient temperature, THF solvent, 18 hours:

Ligand	Solvent	1,2 Addition (%)	1,4 Addition (%)	1,6 Addition (%)	Benzhydrol (%)	Total Yield (%)
TMEDA	THF	2	0	9	1	12
TMEDA	THF	3	0	10	2	15
TMEDA	THF	3	0	13	1	17

7.5 Variation of the *tert*-butyl ligand source

Dpa(H) (0.34 g, 2 mmol) was added to a freshly prepared suspension of ⁿBuNa (0.16 g, 2 mmol) in hexane (6 mL). PMDETA (0.42 mL, 2 mmol) was subsequently introduced, followed by either ^tBu₂Zn (2 mL of a 0.5 M solution in hexane, 1 mmol), or ^tBuLi (1.18 mL of a 1.7 M solution in pentane, 2 mmol). Following the addition of benzophenone (0.18 g, 1 mmol), the reaction was stirred at ambient temperature for 18 hours prior to work up according to Method A.

Stoichiometric reaction conditions, ambient temperature, hexane solvent, 18 hours:

Ligand	Solvent	1,2 Addition (%)	1,4 Addition (%)	1,6 Addition (%)	Benzhydrol (%)	Total Yield (%)
Dimer + 2 ^t BuLi	Hexane	0	0	0	16	16
Dimer + 2 ^t BuLi	Hexane	0	0	0	24	24
Dimer + 2 ^t BuLi	Hexane	0	0	1	26	27
Dimer + 2 ^t BuLi	Hexane	2	0	5	32	39

References

1. G. Sorin, R. M. Mallorquin, Y. Contie, A. Baralle, M. Malacria, J. P. Goddard and L. Fensterbank, *Angew. Chem. Int. Ed.*, 2010, **49**, 8721-8723.
2. M. Valentini, P. S. Pregosin and H. Ruediger, *Organometallics*, 2000, **19**, 2551-2555.
3. A. Macchioni, G. Ciancaleoni, C. Zuccaccia and D. Zuccaccia, *Chem. Soc. Rev.*, 2008, **37**, 479-489.
4. D. Li, I. Keresztes, R. Hopson and P. G. Williard, *Acc. Chem. Res.*, 2009, **42**, 270-280.
5. S. Trefi, C. Routaboul, S. Hamieh, V. Gilard, M. Malet-Martino and R. Martino, *J. Pharmaceut. Biomed.*, 2008, **47**, 103-113.
6. D. R. Armstrong, P. García-Álvarez, A. R. Kennedy, R. E. Mulvey and J. A. Parkinson, *Angew. Chem. Int. Ed.*, 2010, **49**, 3185-3188.
7. D. R. Armstrong, W. Clegg, P. García-Álvarez, M. D. McCall, L. Nuttall, A. R. Kennedy, L. Russo and E. Hevia, *Chem. Eur. J.*, 2011, **17**, 4470-4479.
8. D. R. Armstrong, A. R. Kennedy, R. E. Mulvey, J. A. Parkinson and S. D. Robertson, *Chem. Sci.*, 2012, **3**, 2700-2707.
9. C. Su, R. Hopson and P. G. Williard, *Eur. J. Inorg. Chem.*, 2013, **2013**, 4136-4141.
10. C. C. Su, R. Hopson and P. G. Williard, *J. Am. Chem. Soc.*, 2013, **135**, 12400-12406.
11. O. L. Sydora, P. T. Wolczanski, E. B. Lobkovsky, C. Buda and T. R. Cundari, *Inorg. Chem.*, 2005, **44**, 2606-2618.
12. H. Schumann, M. Hummert, A. N. Lukoyanov and I. L. Fedushkin, *Chem. Eur. J.*, 2007, **13**, 4216-4222.
13. The reaction was performed four times. Refer to ESI for further detail.
14. H. Yamataka, Y. Kawafuji, K. Nagareda, N. Miyano and T. Hanafusa, *J. Org. Chem.*, 1989, **54**, 4706-4708.
15. ZnI possesses a τ_4 value of 0.84, according to the method proposed by Houser. The value of τ_4 represents a scale where 0.00 refers to an ideal square planar geometry, and 1.00 indicates an ideal tetrahedral geometry. , L. Yang, D. R. Powell and R. P. Houser, *Dalton Trans.*, 2007, **36**, 955-964.
16. F. A. Cotton, L. M. Daniels, G. T. Jordan IV and C. A. Murillo, *Polyhedron*, 1998, **17**, 589-597.
17. Y. Gultneh, A. R. Khan, D. Blaise, S. Chaudhry, B. Ahvazi, B. B. Marvey and R. J. Butcher, *J. Inorg. Biochem.*, 1999, **75**, 7-18.
18. K.-Y. Ho, W.-Y. Yu, K.-K. Cheung and C.-M. Che, *Dalton Trans.*, 1999, 1581-1586.
19. S. H. Rahaman, D. Bose, H. Chowdhury, G. Mostafa, H.-K. Fun and B. K. Ghosh, *Polyhedron*, 2005, **24**, 1837-1844.
20. D. R. Armstrong, J. A. Garden, A. R. Kennedy, R. E. Mulvey and S. D. Robertson, *Angew. Chem. Int. Ed.*, 2013, **52**, 7190-7193.
21. H. Gornitzka and D. Stalke, *Eur. J. Inorg. Chem.*, 1998, 311-317.
22. Z. Zheng, M. K. Elmkaddem, C. Fischmeister, T. Roisnel, C. M. Thomas, J.-F. Carpentier and J.-L. Renaud, *New J. Chem.*, 2008, **32**, 2150-2158.
23. M. J. Frisch, G. W. Trucks, H. B. Schlegel, G. E. Scuseria, M. A. Robb, J. R. Cheeseman, J. A. Montgomery, Jr., T. Vreven, K. N. Kudin, J. C. Burant, J. M. Millam, S. S. Iyengar, J. Tomasi, V. Barone, B. Mennucci, M. Cossi, G.

- Scalmani, N. Rega, G. A. Petersson, H. Nakatsuji, M. Hada, M. Ehara, K. Toyota, R. Fukuda, J. Hasegawa, M. Ishida, T. Nakajima, Y. Honda, O. Kitao, H. Nakai, M. Klene, X. Li, J. E. Knox, H. P. Hratchian, J. B. Cross, V. Bakken, C. Adamo, J. Jaramillo, R. Gomperts, R. E. Stratmann, O. Yazyev, A. J. Austin, R. Cammi, C. Pomelli, J. W. Ochterski, P. Y. Ayala, K. Morokuma, G. A. Voth, P. Salvador, J. J. Dannenberg, V. G. Zakrzewski, S. Dapprich, A. D. Daniels, M. C. Strain, O. Farkas, D. K. Malick, A. D. Rabuck, K. Raghavachari, J. B. Foresman, J. V. Ortiz, Q. B. Cui, A.G., S. Clifford, J. Cioslowski, B. B. Stefanov, G. Liu, A. Liashenko, P. Piskorz, I. Komaromi, R. L. Martin, D. J. Fox, T. Keith, M. A. Al-Laham, C. Y. Peng, A. Nanayakkara, M. Challacombe, P. M. W. Gill, B. Johnson, W. Chen, M. W. Wong, C. Gonzalez and J. A. Pople, *GAUSSIAN03 (Revision C.02)*, Gaussian, Inc.: Wallingford, CT, 2004.
24. W. Kohn, A. D. Becke and R. G. Parr, *J. Phys. Chem.*, 1996, **100**, 12974-12980.
 25. A. D. Becke, *Phys Rev A*, 1988, **38**, 3098-3100.
 26. A. D. Mclean and G. S. Chandler, *J. Chem. Phys.*, 1980, **72**, 5639-5648.
 27. R. Krishnan, J. S. Binkley, R. Seeger and J. A. Pople, *J. Chem. Phys.*, 1980, **72**, 650-654.
 28. H. Schödel, C. Näther, H. Bock and F. Butenschön, *Acta Crystallogr.*, 1996, **B52**, 842-853.
 29. J. E. Johnson and R. A. Jacobsen, *Acta Crystallogr.*, 1973, **B29**, 1669-1674.
 30. G. J. Pyrka and A. A. Pinkerton, *Acta Crystallogr.*, 1992, **C48**, 91-94.